Diels-Alder Click Cross-Linked Hyaluronic Acid Hydrogels for Tissue Engineering

by

Chelsea Marlene Nimmo

A thesis submitted in conformity with the requirements
for the degree of Master of Science

Department of Chemistry
University of Toronto

Diels-Alder Click-Crosslinked Hyaluronic Acid Hydrogels for Tissue Engineering

Chelsea Nimmo

Master of Science

Department of Chemistry
University of Toronto

2011

Abstract

Hyaluronic acid (HA) is a naturally occurring polymer that holds considerable promise for tissue engineering applications. Current cross-linking chemistries often require a coupling agent, catalyst, or photoinitiator, which may be cytotoxic, or involve a multistep synthesis of functionalized-HA, increasing the complexity of the system. With the goal of designing a simpler one-step , aqueous-based cross-linking system, we synthesized HA hydrogels via Diels-Alder "click" chemistry. Furan-modified HA derivates were synthesized and cross-linked via dimaleimide poly(ethylene glycol). By controlling the furan to maleimide molar ratio, both the mechanical and degradation properties of the resulting Diels-Alder cross-linked hydrogels can be tuned. Rheological and degradation studies demonstrate that the Diels-Alder click reaction is a suitable cross-linking method for HA. These HA cross-linked hydrogels were shown to be cytocompatible and may represent a promising material for soft tissue engineering.

Acknowledgments

I would like to express my sincere gratitude to my supervisor, Dr. Molly Shoichet for her continued advice and encouragement during my Master's degree. Her passion for academic research has greatly influenced my desire to attack complex scientific questions within my thesis work. It has been a great pleasure to work with all the members of the Shoichet research team, but in particular I would like to single out Dr. Shawn Owen for all his contributions and insights to the project. Lastly, I would like to thank my family and friends for their support during the last two years. I would also like to convey thanks to NSERC and the CIHR Training Program in Regenerative Medicine for my funding.

Table of Contents

List of Tables

List of Figures

List of Schemes

List of Abbreviations

^{1}H HR-MAS NMR	High resolution magic angle spinning proton nuclear magnetic resonance
^{1}H NMR	Proton nuclear magnetic resonance
3D	Three-dimensional
cp	Cyclopentadiene
CS	Chondroinin sulfate
Cu(I)	Copper
CuAAC	Copper(I)-catalyzed alkyne-azide cycloaddition
CuSO4	Copper sulfate
Cys	Cysteine
DMTMM	4-(4,6-Dimethoxy-1,3,5-triazin-2-yl)-4-methmorpholinium chloride
D_2O	Deuterated water
DPBS	Dulbecco's phosphate buffered saline
DS	Degree of substitution
ECM	Extracellular matrix
EDCI	1-[3-(dimethylamino)propyl]-3-ethylcarbodiimide hydrochloride
EDTA	Ethylenediaminetetraacetic acid
FBS	Fetal bovine serum
FTase	Farnesyl transferase
FTIR	Fourier transform infrared
G'	Shear elastic modulus
HA	Hyaluronic Acid
HA-furan	Furan-modified hyaluronic acid derivative
KBr	Potassium bromide
M_0	Pre-swelled hydrogel mass
M_s	Pre-degradation hydrogel mass
M_t	Hydrogel mass at time t
MES	2-(*N*-Morpholino)-ethanesulfonic acid
MI	Maleimide
$(MI)_2PEG$	Bis-maleimido-poly(ethylene glycol)
MMPs	Matrix metalloproteinase's
MSCs	Mesenchymal stem cells
MW	Molecular weight
NSPC	Neural stem/progenitor cell
OGP	Osteogenic growth peptide
PBS	Phosphate buffered saline
PEG	Poly(ethylene glycol)
RGD	Fibronectin tripeptide sequence, arginine-glycine-aspartate
PDGF-AA	Platelet-derived growth factor AA
pCuAAC	Photoinducible azide-alkyne cycloaddition
PVA	Poly(vinyl alcohol)
SAMs	Self-assembled monolayers
SPAAC	Strain-promoted alkyne-azide coupling
Vs	Vinyl sulfone

List of Appendices

1 Introduction

1.1 Hydrogels for Tissue Engineering

Tissue engineering has been defined as the delivery of biomolecules, cells and supporting structures to the body to promote self-healing[1]. In a common approach, tissue-specific cells are isolated from a patient via a small tissue biopsy and subsequently harvested in vitro. These cells are then incorporated into biocompatible 3-dimensional (3D) polymer scaffolds to provide structural support for tissue regeneration in an environment analogous to that of the native extracellular matrix (ECM). These polymer scaffolds then serve as delivery vehicles to distribute the regenerated cells to the patient's body, while providing a space for new tissue formation (**Figure 1**)[2]. Using this approach, many tissues have been successfully engineered, such as bladder, skin, cartilage and bone, of which many are in clinical use[3].

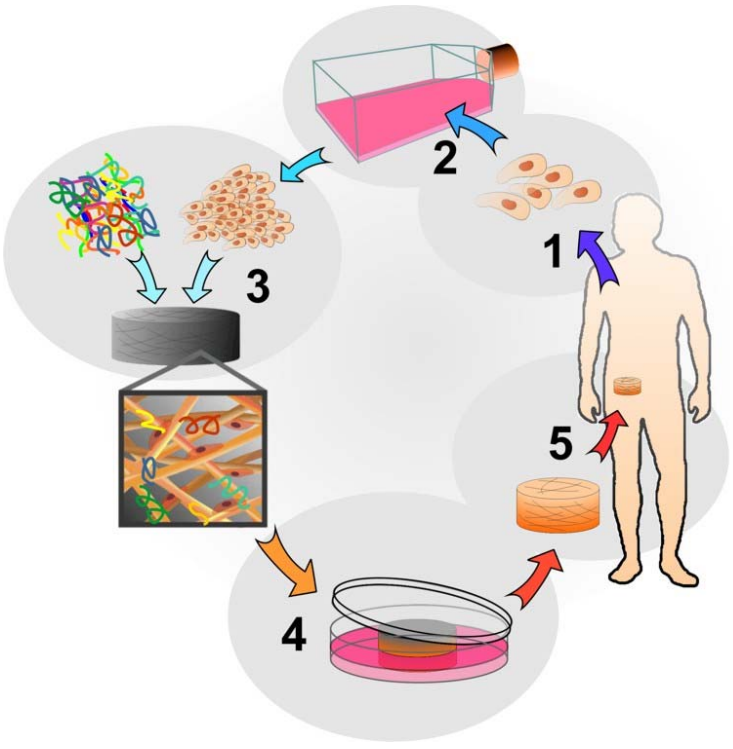

Figure 1. Schematic illustration of a typical tissue engineering approach[2]. Cells are obtained from a patient via a small biopsy and expanded in vitro, and subsequently implanted into a following incorporation with a polymer scaffold.

Among the scaffold materials employed within tissue engineering strategies, hydrogels have gained increasing popularity within the last decade. Hydrogels are water-swollen, cross-linked polymer networks capable of imitating the mechanical and architectural nature of the cellular microenvironment of soft tissue[4]. Due to their high water content, hydrogels permit facile transport of oxygen, nutrients, soluble factors and waste. Moreover, many hydrogels are biocomtatible, biodegradable, and can be synthesized and processed under relatively mild conditions. Accordingly, hydrogels represent an optimal platform for many regenerative medicine applications.

1.1.1 Design Criteria

Hydrogels for tissue engineering applications are generally divided based on their natural or synthetic origin. Given that natural materials are often principle components of the ECM, they bestow many desirable biological properties within the hydrogel scaffold. Common natural materials employed for hydrogel formation include collagen, hyaluronic acid (HA), and fibrin. These hydrogels are bioactive, biocompatible and can promote cell function. On the other hand, hydrogels formed from synthetic materials, such as poly(ethylene glycol) (PEG), and poly(lactic acid), offer a blank canvas, permissive to cell function[4]. These macromolecules are generally easier to work with chemically compared to their naturally-derived counterparts which often exhibit batch-to-batch variability[3]. While there has been considerable debate as to which class of material is superior for tissue engineering applications, many believe the intrinsic cellular interaction and fundamental cell-controlled degradation of native hydrogels make them superior biomimetic scaffolds for ultimate control of cell fate in 3D.

To control tissue regeneration in 3D, many hydrogel design parameters must be considered, besides the choice of polymer. The mechanical properties of a hydrogel scaffold are particular important given that stem cell fate has shown to be regulated according to matrix elasticity[5]. For example, when mesenchymal stem cells (MSCs) were cultured on collagen-coated gels with elastic moduli ranging from either 0.1-1, 8-17, or 25-40 kPa they differentiated into neurons, myogenic cells, or osteoblasts respectively[6]. Mammary epithelia[7] and glioblastomas[8] also exhibit a dependence on matrix rigidity. In addition to the mechanical properties of a hydrogel scaffold, the degradation profile is also important in directing cell behavior. Cells must be able to remodel their environment to ensure adequate tissue regeneration. Mooney and co-workers explored the

influence of matrix degradation on myoblast phenotype[9]. While myoblasts cultured in the non-degradable gels experience the fastest proliferation rate, only cells cultured in degradable gels were able to differentiate into multi-nucleated myofibers.

1.1.2 Hyaluronic Acid Hydrogels

HA is a naturally occurring linear polysaccharide that has repeating units of ß-1,4-D-glucuronic acid and ß-1,3,-*N*-acetyl-D-glucosamine (**Figure 2)**. HA is a non-sulfated glycosaminoglycan, found ubiquitously through the ECM, with reported roles in embryonic development, tissue organization, wound healing, and angiogenesis[10]. HA is also biocompatible, biodegradable, and elicits low levels of immune response[61], and as such as been in clinical use for over 30 years[11]. As mentioned above, natural polymers carry built-in cellular interactive properties and can be degraded in a cell-mediated fashion. Cellular interaction with HA is facilitated by the receptors CD44 and RHAMM[12], and HA is rapidly degraded within the body via hyaluronidase with half-lives ranging from hours to days[13].

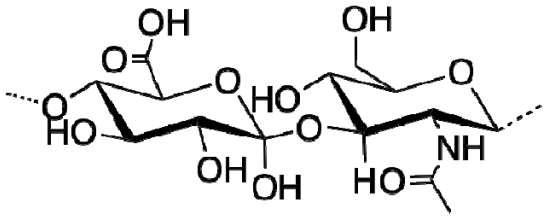

Figure 2. Chemical structure of hyaluronic acid

Recently, HA has been recognized as an important biomaterial for tissue engineering and regenerative medicine applications[14]. Over the past decade, a wide variety of HA-based hydrogels have been engineered, demonstrating dural repair[62], sustained cell expansion[63,64], facilitated cartilage repair[65], oriented bone regeneration[66], and directed neural progenitor cell differentiation[67], among others. HA hydrogels have been cross-linked via photo-polymerization to encapsulate chondrocytes within the hydrogel networks, promoting cartilage regeneration[15]. Redox-initiated HA hydrogels have been used in cardiac repair[16], and photocross-linked HA hydrogels have been explored as biological substitutes for injured heart valves[17]. Furthermore, HA hydrogels have been used as platform to direct stem cell behavior within a 3D environment. Both MSCs[18] and human embryonic stem cells[19] have been encapsulated within HA hydrogels and their ability to self-renew and differentiate has been investigated.

These scaffolds can be manipulated to mimic aspects of the extracellular microenvironment. For example, inclusion of cell-adhesive peptides (RGD)[68] and ECM proteins (collagen)[69] within HA scaffolds can enhance cellular attachment and spreading. Other polymer molecules, such as poly(ethylene glycol) (PEG)[65,68] have also been included in HA hydrogels to vary the mechanical properties and pore size of the scaffolds.

1.1.3 HA Cross-Linking Chemistries

Native HA is water-soluble and exhibits a fast degradation profile and clearance within the body[10,70]. Therefore HA must be covalently cross-linked in order to provide a mechanically robust hydrogel. In the past, popular hydrogel cross-linking methodologies included radical polymerization, chemical reactions of complementary functionalities, or high energy irradiation[20]. Cross-linking typically involves chemical modification of HA by targeting either the hydroxyl or carboxylic acid functionalities of the sugar moieties. For example, HA has been modified with mono- and polyvalent hydrazides, which in turn react with PEG-dialdehydes to form hydrogels[71]. This methodology has been extended with Huisgen click chemistry by crosslinking HA-azide and HA-alkyne derivates under copper catalysis[31]. HA hydrogels have also been synthesized using photo-chemistry with methacrylate-fuctionalized HA and photocross-linkers (Irgacure 2959 or eosin Y)[63,72]. Therefore a coupling agent, catalyst or photo-initiator is often required for cross-linking, introducing potentially cytotoxic small molecules, and hence lowering the biocompatibility of the material. These hydrogels must be extensively washed to remove catalysts or unreacted coupling agents before the addition of cells. This is a laborious process that can lead to undesired hydrogel degradation.

Thiolated-HA can be cross-linked without additives via disulfide bond formation upon oxidation[73]; however, synthesis of thiolated-HA is a time-consuming, multi-step process that can negatively impact the native structure of HA by decreasing the molecular weight. Moreover, inclusion of thiols in the HA backbone may complicate cross-linking reactions in the presence of cysteine-containing peptides or proteins. These may react with HA-thiols, resulting in disulfide bond formation, thereby affecting their structure and function. Furthermore, thiol-disulfide oxidoreduction of cell surface proteins plays a role in regulating critical cellular functions such as adhesion and proliferation[76], and thus a blank hydrogel canvas without thiols allows more control over cellular behavior.

1.2 Click Chemistry within Regenerative Medicine

Tissue engineering strategies require well-defined structural materials. Recognizing this fact, many bioengineers have turned to synthetic organic techniques for their cross-linking reactions. The exponential growth of click chemistry research within the past decade has greatly facilitated the development of chemoselective chemistries applicable within biomaterials. In 2001, Sharpless and co-workers introduced the term "click chemistry" to define a set of nearly perfect reactions that resemble natural biochemical ligations[21]. These "spring-loaded" reactions are orthogonal, regioselective, and highly efficient. Moreover, click reactions can be performed in aqueous solutions at room or physiological temperature, and display outstanding functional group tolerance, making them compelling reactions within the bioengineering toolkit for polymer synthesis and bioconjugation[22]. Accordingly, there has been an emerging trend of click chemistry within the field of regenerative medicine. A prime example is click cross-linked hydrogels. Click reactions have also gained popularity as bioconjugation techniques for decorating 2D cell substrates, as elegant patterning chemistries for immobilizing bioactive factors within 3D scaffolds (**Figure 3**). This section begins with a brief overview of three common click reactions employed within regenerative biomaterials, and further highlights their use in tissue engineering and regenerative medicine.

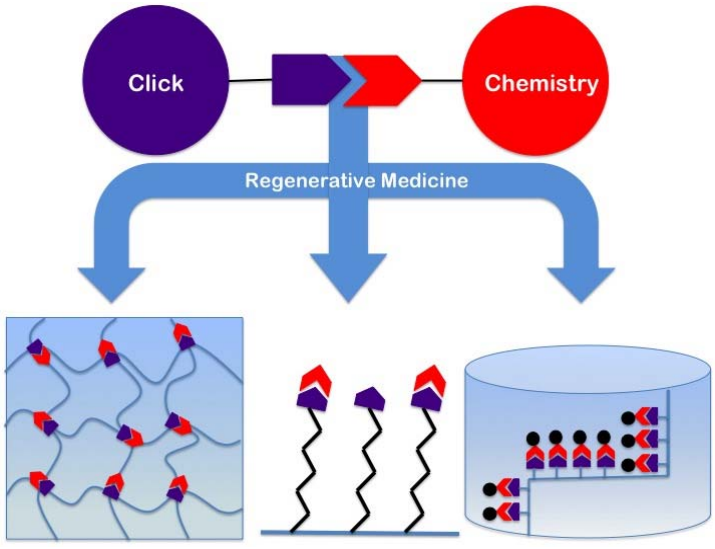

Figure 3. Schematic representation of click chemistry applied to regenerative biomaterials. Click chemistry has been employed as a crosslinking chemistry for hydrogel synthesis, and as bioconjugation techniques for decorating 2D cell culture substrates and patterning bioactive factors within 3D scaffolds.

1.2.1 Common Click Reactions in Regenerative Biomaterials

The term click chemistry often refers to the common copper(I)-catalyzed alkyne-azide cycloaddition (CuAAC) (**Scheme 1A**). This reaction is very similar to the classic Huisgen cycloaddition[23] where an organic azide reacts with an alkyne to form a triazole ring. Through the addition of a Cu(I) catalyst, Meldal[24] and Sharpless[25] demonstrated that the Huisgen cycloaddition reaction can proceed at low temperatures with high rates, efficiency, and regiospecificity. Moreover, near-perfect conversion is obtainable in both aqueous and organic solvents. CuAAC has proved to be particularity advantageous within biomedical applications considering the starting materials, azides and terminal alkynes, are remarkably stable within biological systems, enabling facile introduction of these reactive groups into a wide range of biomolecules.

However, the term click chemistry is not limited to the CuAAC reaction, but embodies a synthetic philosophy of many reactions with distinct mechanisms. According to Sharpless, a reaction can achieve click status if it consists of readily available orthogonal reactants that combine under mild conditions to produce a single stereospecific product, with little or no isolation[21]. Within the past decade there has been increasing investigation into reactions that meet this definition, yet do not require a metal catalyst[34]. The Bertozzi lab has developed a reaction of azides with cyclooctyne derivatives[35] referred to as strain-promoted azide-alkyne coupling (SPAAC) (**Scheme 1B**). These cyclooctyne derivatives greatly increase reactivity of azide-alkyne cycloadditions in the absence of copper, particularly when difluorinated[36]. Baskin et al. exploited this phenomenon to conjugate fluorophores to biological molecules by incorporating a *gem*-difluoro group next to a strained alkyne[37]. Reported reaction rates were 30-60 times faster compared to those with non-fluorinated cyclooctynes.

Another click cycloaddition is exemplified by the Diels-Alder (DA) reaction; a highly selective [4 + 2] cycloaddition between an electron-rich diene and an electron-poor dienophile (**Scheme 1C**). This reaction was first reported by Otto Diels and Kurt Alder in 1928[48], making the DA cylocaddition the oldest known click reaction. DA chemistries offer high yields and minimal sides reactions, and require very little energy. Contrary to other click reactions, which commonly result in carbon-heteroatom bonds, carbon-carbon bonds are formed in DA cycloadditions. These

bonds are thermally reversible at elevated temperatures. Water has been shown to accelerate DA reactions[49,50], making the DA reaction particularly desirable for biomedical applications.

Beyond cycloadditions, other highly efficient reactions, such as nucleophilic substitutions, radical additions, and Michael additions, are also considered click reactions. In particular, the thiol-ene reaction has recently been identified as a click reaction with specific applications in biofunctionalization and surface modification[40]. Thiol-click coupling by free radical addition and by Michael addition reactions are two principle variations which are often used within the field of regenerative biomaterials (**Scheme 1D**). While both offer high efficiency, photoinitiation of the radical addition reaction between thiols and alkenes allows for spatial and temporal control. The thiol-Michael addition is characterized by thiol-vinyl reactions between a thiol and an electron-deficient 'ene'. A particularly relevant example is thiol-maleimide click coupling (**Scheme 1E**), which is frequently exploited for protein conjugation[92,93,99,100].

Scheme 1. Common click reactions for regenerative biomaterials

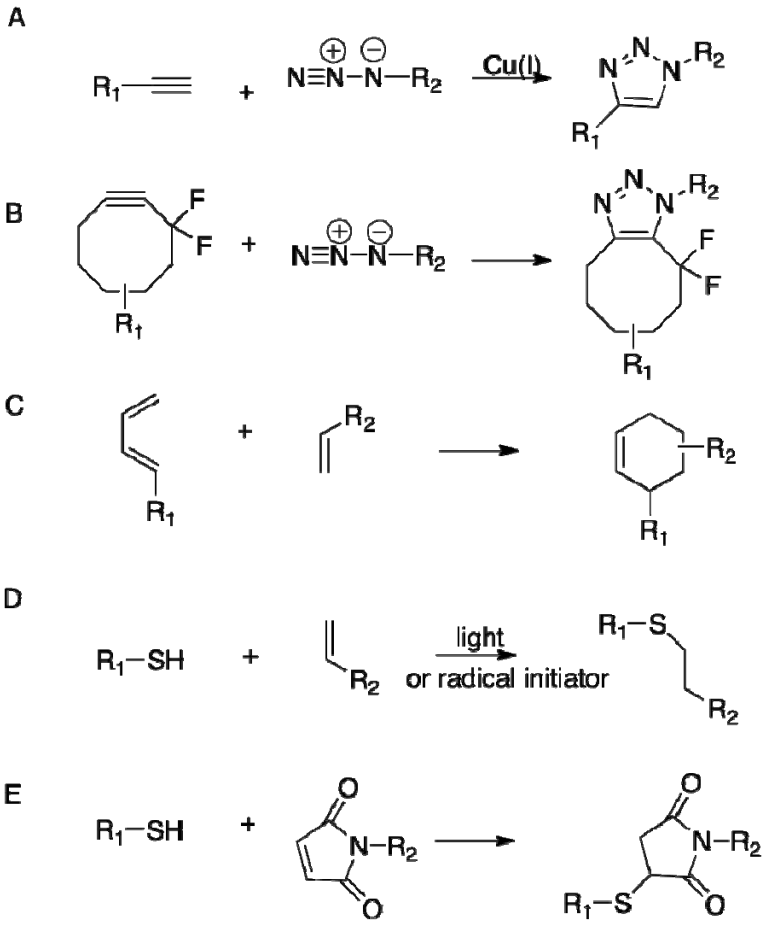

1.2.2 Click Cross-Linked Hydrogels for Tissue Engineering and Drug Delivery

1.2.2.1 Alkyne-Azide Click Cross-Linked Hydrogels

Ossipov et al. were the first to recognize the CuAAC reaction as an efficient chemoselective cross-linking method for hydrogel synthesis[26]. Poly(vinyl alcohol) (PVA) was functionalized with either acetylene or azide groups, and cross-linked by mixing their aqueous solutions together with copper sulfate ($CuSO_4$) and sodium ascorbate as the cycloaddition catalyst. In another example, alkyne-modified PVA was cross-linked with bifunctional PEG-diazide. Hydrogels prepared with polyfunctional PVA formed higher modulus gels with reduced swelling than those synthesized with the bifunctional PEG crosslinker.

Hawker and co-workers[27] applied the CuAAC click cross-linking reaction to the synthesis of pure PEG hydrogels. In their approach, diacetylene- and tetraazide-functionalized PEG were reacted in a 2:1 ratio at room temperature under aqueous conditions in the presence of $CuSO_4$ and sodium ascorbate. By manipulating both the polymer and catalyst concentration, they were able to tune the cross-linking efficiency. Following hydrogel formation, both acetylene and azide functionalized chromophores were swollen into the hydrogel to visualize any residual azide/acetylene functional groups. This revealed a maximum of 0.2% unreacted functional groups, confirming the efficient nature of the CuAAC reaction. The degree of swelling and stress/extension properties of the hydrogels were also examined by varying the length of the diacetylene PEG chain.

To illustrate the fidelity of the CuAAC cross-linked PEG hydrogels as tissue engineering and drug delivery scaffolds, various researchers have incorporated peptides and degradable linkers within their click cross-linked networks. In particular, inclusion of the fibronectin tripeptide sequence, arginine-glycine-aspartate (RGD), has been shown to be an essential additive in almost hydrogel formulations for tissue culture. RGD is a prime cell adhesion site that is recognized by many integrin receptors [28] therefore incorporation of this peptide facilitates cell-matrix interactions. Liu et al. synthesized diazide functionalized RGD peptides to cross-link tetraacetylene PEG under aqueous conditions with $CuSO_4$ and sodium ascorbate[29]. By varying the temperature, catalyst and precursor concentrations, the gelation time was altered from 2 to 30 minutes. An increase in temperature or $CuSO_4$, resulted in a decreased gelation time. The storage

modulus was also tailored by changing the azide linker length. These RGD peptide hydrogels were tested for fibroblast delivery to promote tissue repair. By increasing the concentration of RGD peptide, fibroblast adhesion and proliferation also increased.

In a similar approach, van Dijk et al. incorporated a protease-sensitive peptide within a CuAAC cross-linked PEG hydrogel (**Figure 4**)[30]. Alkyne-functionalized star-shaped PEG molecules (either 4- or 8-armed with a MW of 10 and 20 kDa, respectively) were cross-linked with the protease-sensitive bis-azido peptide in aqueous solution in the presence of $CuSO_4$ and sodium ascorbate. Incubation of the hydrogels in trypsin lead to completely degraded hydrogels after 40-80 hours, depending on the cross-link density. Again, the hydrogel properties could be tailored by several factors, such as the solid content of the hydrogel, or the molecular weight and architecture of the PEG molecules.

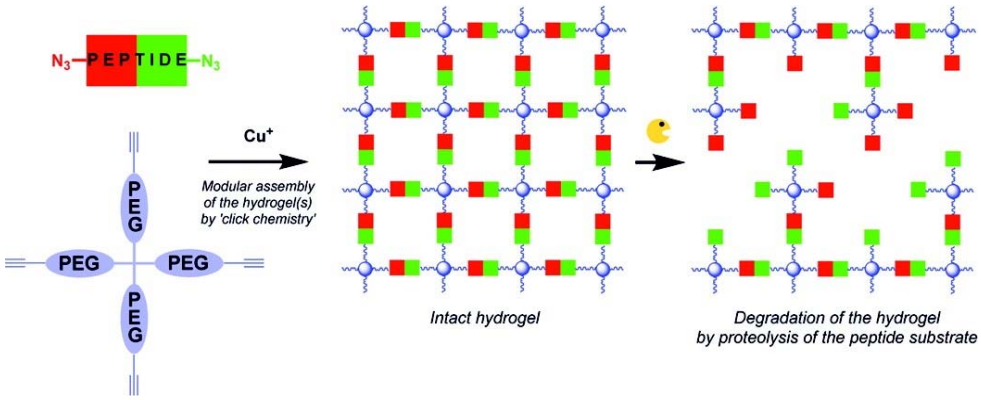

Figure 4. Schematic of the synthesis of CuAAC cross-linked PEG hydrogels[30]. Incorporation of enzymatically degradable peptides renders hydrogels susceptible to degradation by trypsin proteases.

The CuAAC reaction has also been employed as a cross-linking method for natural polymers. Crescenzi et al. used the CuAAC click reaction to cross-link HA[31]. HA was modified with either azide or alkyne groups and cross-linked in water with Cu(I) at room temperature **(Scheme 2)**. Their hydrogel revealed intriguing characteristics for both drug release and tissue engineering applications. As a model for drug delivery, benzidamine and doxorubicin were encapsulated within the click hydrogels, which displayed release profiles ranging from hours to several weeks, depending on the cross-link density. To confirm the possibility that these hydrogels could serve as tissue engineering scaffolds, yeast cells were imbedded within the hydrogels, following removal of the copper catalyst through dialysis. Cells exhibited 80% proliferating activity after

24 hours in culture. In a follow-up study, the influence of the dialkyne structure on the properties of these HA click cross-linked hydrogels was examined[32]. HA azido-derivatives cross-linked with shorter dialkynes experienced weaker storage moduli, corresponding with predicted cross-linking densities as determined by NMR.

Scheme 2. Synthesis of CuAAC cross-linked HA hydrogels[31]

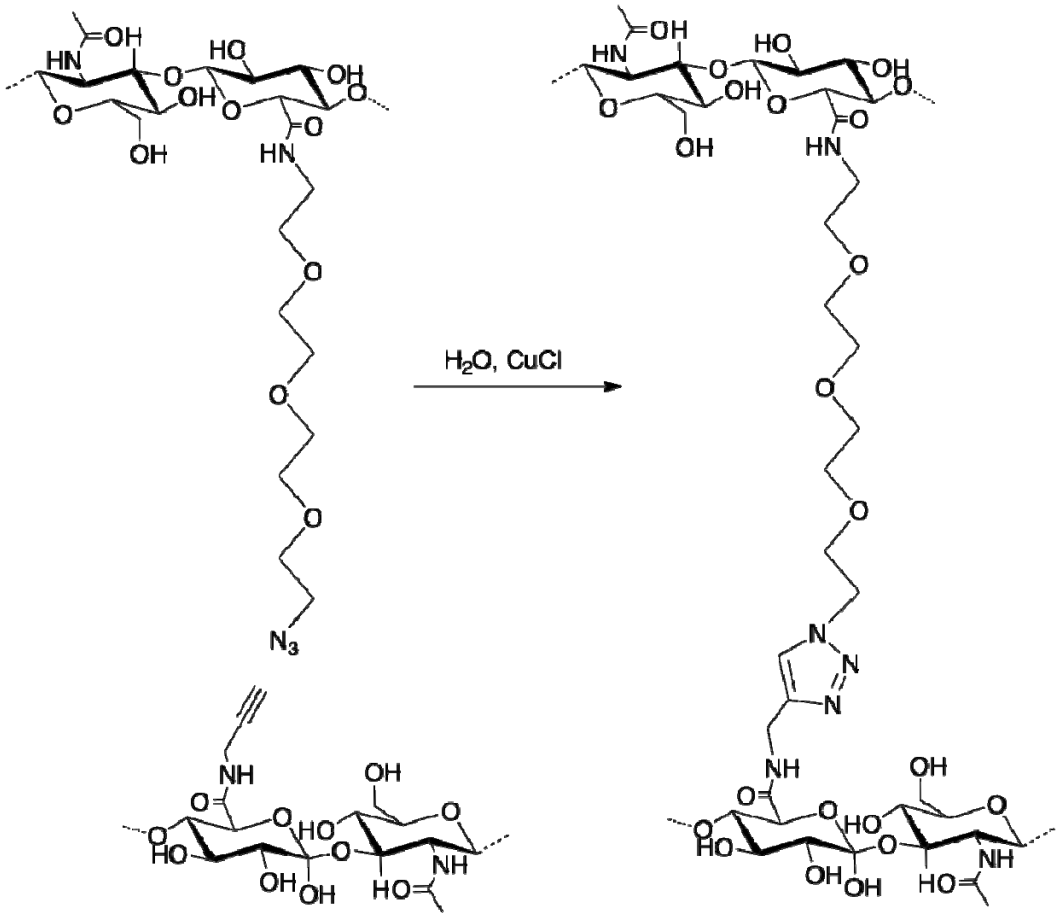

Gao and co-workers also employed the CuAAC reaction to cross-link natural biopolymers[33]. Both HA and chondroinin sulfate (CS) were modified to contain azide functionalities, and cross-linked with gelatin that had been modified with an alkyne functionality. They argue this triple co-polymer system better mimics the natural components of ECM by incorporating proteoglycans such as CS, and denatured collagen products, such as gelatin, to promote cell surface adhesion. Aqueous solutions of the polymers were combined and catalyzed by Cu(I) to form a hydrogel with the time to gelation varying as a function of catalyst concentration. Chondrocytes were cultured in vitro to assess the cytotoxicity of the click hydrogels. After 3

days in culture, a confluent layer of cells had formed, confirming the benefit of this click cross-linked hydrogel for chondrocyte adhesion and proliferation.

Anseth and co-workers have gone beyond traditional CuAAC cross-linking chemistry and synthesized PEG hydrogels via SPAAC, to bestow copper-free, physiological conditions within their networks[38]. In their approach, a four-arm PEG tetra-azide was reacted with difunctionalized di-fluorinated cyclooctyne polypeptide sequence, to incorporate enzymatically degradable cross-linker sequences throughout the material. Gelation occurred in less than 5 minutes, and both rheological and NMR data support the ideality of the network, similar to previous click-based networks[27]. This click strategy tolerates cell encapsulation with high viabilities (>90% at 24 hours). As an extension of this study, De Forest et al. enabled control over cross-link density and shear moduli of these SPAAC cross-linked PEG hydrogels[39]. By altering either the azide:cyclooctyne ratio, or the molecular weight of PEG, hydrogels were synthesized with tunable moduli ranging from 1000 – 6000 Pa. These SPAAC cross-linked PEG hydrogels have also served as patterning platforms for the immobilization of biological functionalities using thiol-ene click photocoupling[38,39]. (see Click Patterning of 3D Scaffolds section)

A drawback of CuAAC cross-linking is the lack of temporal and spatial control due to the generation of the catalytic Cu(I) species[101]. Spatial and temporal control of network formation is paramount in many tissue engineering applications. To overcome this, Adzima et al. sought to catalyze the CuAAC cross-linking reaction via the photochemical reduction of Cu(II) to Cu(I)[101]. Generating Cu(I) photochemically is analogous to the initiation of a radical or carbocation species in traditional photopolymerization processes, resulting in total spatial and temporal control of the CuAAC reaction. The authors developed this photoinducible azide-alkyne cycloaddtion (pCuAAC) reaction to synthesize hydrogels by irradiating multifunctional alkyne and azide functionalized PEG monomers in the presence of $CuSO_4$ and Irgacure 2959 photoinitiator. To extend this system to biological systems, the authors suggest modifications to mimic reverse-ATRP polymerizations that require significantly lower copper levels[102].

1.2.2.2 Thiol-Click Cross-Linked Hydrogels

Qiu et al. were the first to harness the thiol-Michael click reaction for hydrogel formation[41]. PEG-based copolymers containing multiple thiol functionalities were cross-linked via divinylsulfone-PEG in neutral phosphate buffer. This system proved to be bioorthogonal, as

protein additives did not interfere with the click cross-linking reaction; however, these proteins did not contain any exposed thiols that could interfere with the reaction. A thiol-click cross-linked hydrogel may be inappropriate for protein delivery if any free thiol groups are present on the proteins. Notwithstanding this limitation, when proteins were incorporated into these gels, their release was sustained for 2-4 weeks.

Hubbell and co-workers took advantage of this Michael-type addition click reaction to synthesize hydrogels with characteristics similar to that of native ECM[42]. Their approach was to incorporate integrin-binding sites for cell adhesion and enzyme-degradable sites into the matrix such that cell-secreted matrix metalloproteinases (MMPs) would enable cell migration into and remodeling of the biomimetic ECM[43]. To achieve this they cross-linked bis-cysteine MMP substrate peptides with vinyl sulfone-functionalized multiarm PEG. The resulting click hydrogel networks displayed a defined molecular architecture, and allowed for invasion by primary human fibroblasts. Cellular invasion was shown to be dependent on the proteolytic activity of the incorporated peptide. The hydrogels were also employed as a drug delivery vehicle for recombinant human bone morphogenetic protein (BMP2) to rat cranium defects. As was observed with their in vitro work for cell penetration, the susceptibility of the enzyme cross-linked hydrogel to cell secreted MMPs, impacted in vivo bone regeneration.

Chawla et al. recently developed a 3D cell culture platform for MSCs by cross-linking a saccharide-peptide copolymer via Michael-type conjugation addition between cysteine (Cys) and vinyl sulfone (VS)[44]. By altering the pH of the cross-linking reaction, or the VS:Cys ratio, they were able to tune both the degradation and mechanical properties of the gel. Hydrogels that were cross-linked with an equimolar ratio of VS:Cys maintained their mechanical stability for longer than 21 days in vitro, similar to dextran hydrogels cross-linked by Michael addition[45]. Their hydrogels also exhibited a rapid gelation time, suggesting utility for in situ surgical procedures, and displayed a microporous network when visualized under environmental scanning electron microscopy. The cell encapsulation was facilitated by the cross-linking reaction occurring in the culture medium. MSCs remained viable after 14 days (>90%) in culture.

The radical-mediated thiol-ene click reaction has also been employed as a hydrogel cross-linking method. Anseth and co-workers developed a platform for hydrogel synthesis by a step-growth reaction mechanism via thiol and norbornene functionalities[46]. Not always achievable with

simple Michael addition, thiol-ene photopolymerization offers spatial and temporal control of network formation. Hydrogels were synthesized by mixing norbornene-functionalized PEG with either chymotrypsin- or MMP-degradable linkers in a 1:1 stoichiometric ratio in PBS. The networks maintained high cell viability following encapsulation (>95% following 24 hours). Anderson et al. utilized these thiol-ene photopolymerized PEG hydrogels to examine MSC behavior in response to network properties[47]. Both MMP cleavable peptide linkers and non-degradable PEG-dithiol linkers were incorporated into the hydrogel to monitor how MSC degradation of the matrix affects their behavior. Their findings suggest directed chondrogenic and adipogenic differentiation of MSCs are facilitated by increased cell-mediated hydrogel degradation.

1.2.2.3 Diels-Alder Click Cross-Linked Hydrogels

Although the Diels-Alder click reaction has long served as an exceptional cross-linking method for the synthesis of complex polymer networks[51-54], the preparation of cross-linked hydrogels via Diels-Alder chemistry remains largely unexplored. A few Diels-Alder hydrogels have been synthesized with synthetic polymers[55-58]; however, these studies have mainly examined the effect of temperature on gelation time and on the retro-Diels-Alder reaction.

1.2.3 Click Immobilization of Peptides on 2D Surfaces

Well-defined chemically modified substrates, such as self-assembled monolayers (SAMs), serve as investigative tools to explore fundamental interactions applicable to regenerative strategies. Surface functionalization is particularly advantageous when engineering substrates for cell culture to harness control over cell-matrix interactions. Many have employed this strategy to immobilize ECM-derived biomolecules for ultimate characterization of their effects on cell adhesion[103-106]. Popular immobilization strategies in the past have been based on adsorption or covalent modification of a protein's functional group(s) to a chemically activated surface[107-108]. These methods can result in side reactions and are difficult to characterize both physically and in terms of cellular response. Accordingly, there has been a paradigm shift in the existing approaches for surface functionalization from unspecific and nonselective reactions towards highly specific orthogonal reactions that ensure bioactivity and facilitate characterization of engineered surfaces[109].

1.2.3.1 CuAAC Click Immobilization

CuAAC is chemoselective against common functionalities in biomolecules, and thus stable reactive species can be introduced within biomolecules with ease. Accordingly, CuAAC serves as an effective click reaction to chemoselectively immobilize peptides to otherwise bioinert SAMs. Becker and co-workers developed a universal technology for surface conjugation of any biomolecule containing accessible azide groups[110]. SAMs were subjected to oxidation by UV exposure, creating a monotonically increasing carboxyl density gradient. A bifunctional propargyl-functionalized linker was then attached to the carboxylic moieties of the gradient to yield an alkyne gradient, making it susceptible to modification with any azido-derivatized species via CuAAC chemistry. The authors tested their methodology by conjugating the RGD tripeptide sequence in a density gradient ranging from 0 to 140 pmolcm^{-2}. Smooth muscle cells cultured on the RGD gradient surfaces revealed enhanced cell attachment with increased RGD concentration. Alkyne-modified KGRGDS has also been successfully coupled by CuAAC chemistry to self-assembled polymeric micelles with azide-functional groups, thereby yielding RGD-functionalized polymeric nanoparticles that specifically bind to corneal epithelial cells[111].

Becker and co-workers later exploited their CuAAC technology to couple osteogenic growth peptide (OGP) to SAMs in order to explore the effects of OGP density on pre-osteoblast cell adhesion, morphology, and proliferation[112]. OGP has been recognized as a promising agent for bone tissue engineering applications because it stimulates tissue regeneration of bone defects[113]. To create the peptide gradient, the carboxylic acid functionalities on the SAM layer were reacted with the amine terminal of a bifunctional amine-poly(ethylene oxide)-alkyne linker, resulting in an alkyne gradient. Azide terminated OGP peptides were then conjugated to the alkyne gradient by immersing substrates in a solution of $CuSO_4$, sodium ascorbate, and peptide for 24 hours at 40 °C. Pre-osteoblast cells were cultured on the OGP functionalized gradient surfaces in serum-free conditions for 7 days. Cell adhesion was highest at low OGP peptide concentrations. At day 3, cells experienced faster doubling rates compared to cells cultured on control surfaces, but this effect subsided by day 7. This is indicative of the natural transition made by osteoblasts from proliferative to maturation phases. Gene expression experiments also verified this phenomena with a 10-fold increase in collagen I expression between days 3 and 7, coinciding with the initial stages of bone mineralization.

Hudalla and Murphy fabricated SAMs expressing a variation of the adhesive RGD peptide, RGDSP, as a means to study stem cell adhesion[103]. This was achieved via CuAAC. SAMs were first prepared by immersing a gold substrate in an ethanolic solution of 80 mol% tri(ethylene glycol) alkanethiolate (HS-EG_3) and 20 mol% azide-terminated hexa(ethylene glycol) alkanethiolate (HS-EG_6-N_3). The resulting mixed SAMs contained approximately 10% HS-EG_6-N_3 and 90% HS-EG_3 (**Figure 5A**); however, this result could be tailored by varying the ratio of HS-EG_6-N_3 and HS-EG_3. The SAMs were classified as bioinert, as they displayed minimal nonspecific protein adsorption. Acetylene-bearing RGDSP (Hex-RGDSP) was then conjugated to the SAMs via HS-EG_6-N_3 in the presence of a Cu(I) catalyst (**Figure 5B**). The CuAAC reaction efficiency illustrated near quantitative conjugation upon the addition of a tertiary amine, which has been a proven method utilized by others to enhance CuAAC efficiency by binding the Cu(I) catalyst[114]. MSCs were cultured on top of the RGDSP-presenting SAMs. RDGSP surface density and intermolecular spacing regulated MSC morphology and attachment (**Figure 5C**).

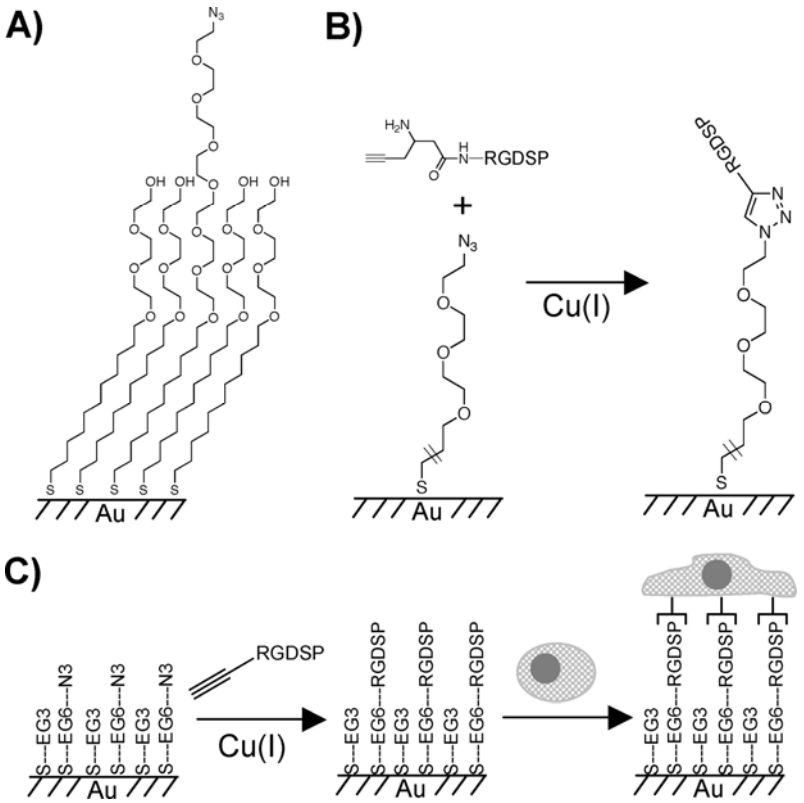

Figure 5. CuAAC click immobilization of peptides to SAM substrates to study stem cell adhesion[103]. **A)** mixed SAMs bearing azide groups; **B)** reaction between azide-functionalized SAMs with acetylene-bearing RGDSP; **C)** the surface density of RGDSP immobilized via CuAAC affects mesenchymal stem cell adhesion and spreading.

In a follow up study, Hudalla and Murphy demonstrated CuAAC conjugation of biomolecules to SAM substrates can be conducted in parallel with other chemistries, namely carbodiimide condensation[115]. Incorporation of carboxylate-terminated hexaethylene glycol alkanethiolate (HS-EG_6-COOH) with the original mixed SAM allowed for conjugation of two distinct peptides, RGDSP and TYRSRKY, a proteoglycan-binding peptide. These experiments revealed that these distinct extracellular factors work synergistically to regulate MSC adhesion on 2D substrates. They also demonstrated that soluble biomolecules, such as heparin, can disrupt specific cell-material interactions, and in turn direct MSC adhesion.

1.2.3.2 Diels-Alder Click Immobilization

Yousaf and Mrksich were the first to exploit the DA reaction for protein immobilization on 2D surfaces[116]. In their approach, SAMs were modified with a hydroquinonequinone group, which upon oxidation provides a quinone, enabling a cycloaddition between the quinone and a cyclopentadiene (cp). To demonstrate this DA approach, they immobilized a biotin-cp conjugate, and tested the affinity of the immobilized biotin for streptavidin. This work demonstrated the DA click reaction is an attractive bioconjugation technique for a wide variety applications, which could be extended to regenerative therapies. The authors also state this method would allow for controlled, sequential immobilization of several biomolecules.

Sun et al. demonstrated the use of sequential click reactions for protein immobilization on solid surfaces[117]. First, the DA click reaction was used to immobilize a heterobifunctional PEG linker carrying alkyne and cyclodiene terminal groups onto an N-(E-maleimidocaproyl)-functionalized glass slide. This resulted in an exposed alkyne-terminated PEGylated surface, vulnerable to conjugation with azide-containing biomolecules via CuAAC click chemistry. Again, biotin was chosen as a model protein for immobilization. Biotin-PEG-azide was added to a glass vial containing the alkyne-PEGylated glass slide, $CuSO_4$, and a tertiary amine ligand. The reaction was left at 4 °C for 12 hours. Biotinylated-glass slides were then immersed in a solution of dilute FITC-conjugated streptavidin at 4 °C for 2 hours. Confocal fluorescence images verified the fidelity of the click protein immobilization. This technique is applicable to a wide range of functionally complex biomolecules for the design of biomimetic surfaces.

1.2.3.3 Thiol-ene Click Immobilization

Waldmann and co-workers reported the use of the thiol-ene reaction to photochemically pattern proteins and other biomolecules onto solid surfaces[118]. Polyamidoamine dendrimers, containing an aminocaproic acid spacer, were covalently attached to a silicon oxide wafer surface. Cystamine was then conjugated to the spacer, which upon disulfide reduction, exposed free thiols on the surface. A solution of terminal-olefin-functionalized biomolecules were spread onto the surfaces, and covered with a photomask. Following irradiation at 365-405 nm, a covalently attached pattern of thioethers was obtained. As a test application, biotin was photochemically patterned onto a thiolated-wafer, and subsequently incubated in a solution of Cy5-labeled streptavidin to render a fluorescent pattern surface. Immobilization was shown to be dependent on irradiation time, and concentration of immobilized peptide. They further exemplified the broad applicability of their patterning method by immobilizing alkaline phosphatase, Ras, and phosphopeptide, all of which retained their bioactivity and binding affinities.

In an extension of this work, Waldmann and co-workers demonstrated fast, oriented covalent immobilization of proteins directly from lysates, eliminating any additional protein chemical modifications[119]. The authors took advantage of the fact that, in cells, many proteins are post-translationally S-farnesylated at a C-terminal "CAAX-box" by protein farnesyltransferase (FTase)[120]. By genetically coding for the CAAX tag, the authors enabled farnesylation *in vitro* or *in vivo* with FTase, creating a facile method for 'ene' incorporation into a protein of interest. Once farnesylated, these proteins were immobilized via the thiol-ene photochemical click reaction to surface-exposed thiols.

1.2.4 Click Patterning of 3D Scaffolds

Throughout the past decade, several scaffolds have emerged aiming to mimic the cellular microenvironment, and ultimately control cell fate and guide tissue regeneration. These scaffolds can be fine-tuned to study a specific parameter of the microenvironment. Notably, the effect of peptide presentation on the cell has been examined by spatially immobilizing proteins and adhesion peptides in 3D patterns within scaffolds. Growth factors localized in 3D scaffolds remain bioactive[121-123] and have been shown to orient axonal growth[92,99], guide cellular migration[91], and cause morphological changes[38]. The stringent spatial resolution and controlled biochemical heterogeneity required for 3D patterning make simple bioorthogonal chemistries

paramount. The use of click reactions for 3D patterning of scaffolds allows significant spatial control when combined with multi-photon processing[93,100]. Additionally, many of these hydrogel scaffolds are click crosslinked, and sequentially click patterned[38,39,124].

1.2.4.1 Alkyne-Azide Click Patterning

Recently, Bowman and co-workers demonstrated 3D patterning of hydrogels via pCuAAC[101]. The transient generation of Cu(I) facilitates spatial and temporal control of the CuAAC reaction. PEG hydrogels were first synthesized by a thiol-yne reaction, ensuring a stoichiometric excess of alkynes. Post-gelation, a solution of photoinitiator (Irgacure 2959), copper sulfate, and an azide-labelled fluorophore was swollen into the gel. Upon irradiation with a photomask, Cu(I) is generated within the irradiated areas, catalyzing the pCuAAC reaction between the azide-fluorophore and the pendant alkynes in the polymer network, ultimately producing a spatially defined fluorescent pattern within the hydrogel. The authors note that future work is required to translate this system to biological systems.

1.2.4.2 Thiol-ene Click Patterned Scaffolds

Immobilization of bioactive growth factors via thiol conjugation has become increasingly popular given the ease of cysteine incorporation within a peptide, making the thiol-ene click reaction particularly relevant for 3D patterning. Anseth and co-workers developed a sequential click protocol relevant to both hydrogel synthesis and post-gelation modification[38,39,124]. Click cross-linked PEG hydrogels were first formed via CuAAC, as an extension of the method taken by Malkock et al[27]. To enable photopatterning of their PEG hydrogels, multifunctional photoreactive polypeptide sequences were included within the network structure by incorporating the non-natural amino acid, Fmoc-Lys(alloc)-OH[124]. The allyloxycarbonyl (alloc) protecting group contains a vinyl functional group capable of reacting with any thiol-containing compound, such as cysteine. Upon exposure to UV light, thiyl radicals are generated via the photocleavage of a hydrogen-abstracting initiator, thereby using light to achieve spatial and temporal control of thiol-ene functionalization within the network. To illustrate this technique, a fluorescently labeled cysteine containing peptide was patterned within PEG hydrogels via transparency-based photolithographic patterning techniques.

This thiol-ene photopatterning method was later employed to immobilize peptides and proteins within PEG hydrogels cross-linked via SPAAC (**Figure 6**)[38]. Spatial and temporal control was validated by selectively exposing certain locations within the hydrogel matrix to light, and by controlling light intensity and exposure time. Furthermore, the thiol-ene reaction was confirmed to be cytocompatible, as 3T3 cells encapsulated within the hydrogel maintained high viability throughout patterning (>90% at 24 h post encapsulation), and thiol-ene immobilization of RGD within the network was shown to influence cell morphology. In a follow-up study, DeForest et al. verified patterning concentration within the hydrogel is directly proportional to the dosage of light, as well as the photoinitiator concentration[39]. Using this system, they were able to construct well-defined 3D biochemical gradients of multiple peptides, offering potential promise to elucidate fundamental biological processes essential to regenerative medicine such as induced cell migration.

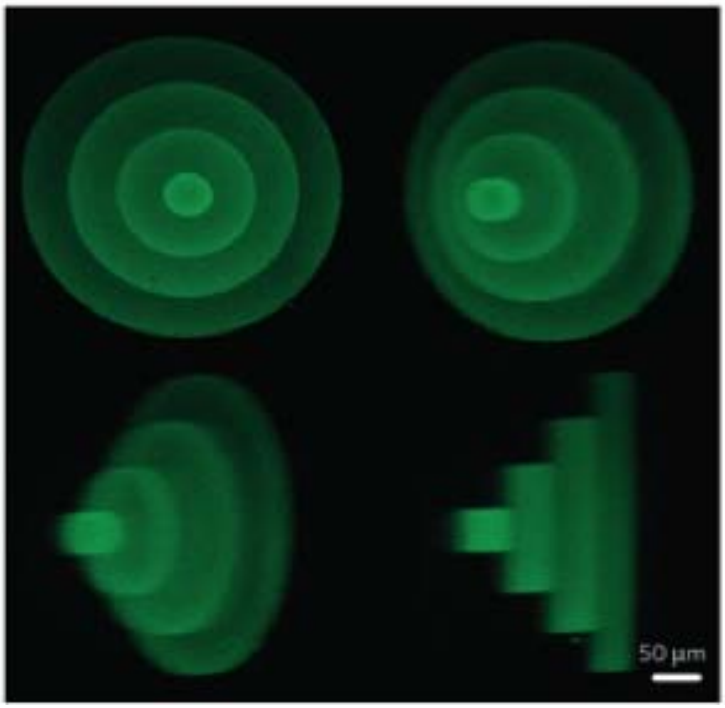

Figure 6. 3D biochemical patterning of PEG hydrogels via thiol-ene photocoupling[38]. Fluorescently tagged peptides were patterned within SPAAC cross-linked networks.

1.2.4.3 Thiol-Maleimide Click Patterning

The thiol-maleimide reaction exemplifies a variation of the thiol-Michael click reaction. Shoichet and co-workers have exploited this click reaction for 3D patterning of agarose hydrogels[92,93,100,121]. Covalent modification of agarose with S-2-nitrobenzyl-cysteine (S-NBC) renders a photolabile matrix, which upon UV irradiation, releases free thiols capable of reacting with any thiol-reactive biomolecule through Michael addition. Thiol-channels were created on exposure to a focused laser beam, and reacted with a maleimide-terminated RGD peptide. This immobilized RGD channel volume promoted neurite extension and cell migration[92]. This system was also applied to study the effect of immobilized platelet derived growth factor AA (PDGF-AA) on neural stem/progenitor cell (NSPC) differentiation[121]. Hydrogels with immobilized RGD and PDGF-AA supported NSPC adhesion and preferential differentiation to oligodendrocytes.

In order to advance this click technology towards more sophisticated architectures that better mimic the native extracellular matrix, agarose was later modified with a coumarin derivative, which upon exposure to a pulsed infrared laser yields free thiols[100]. The use of this photolabile group, allows for intricate 3D control by way of multi-photon excitation. Aizawa et al. exploited this coumarin multi-photon patterning technique to immobilize a gradient of the angiogenic factor, VEGF165, within agarose hydrogels[93]. Primary endothelial cells responded to this immobilized gradient by displaying tip and stalk cell morphology, eventually forming tubule-like structures as they migrated in response to the VEGF gradient (**Figure 7**).

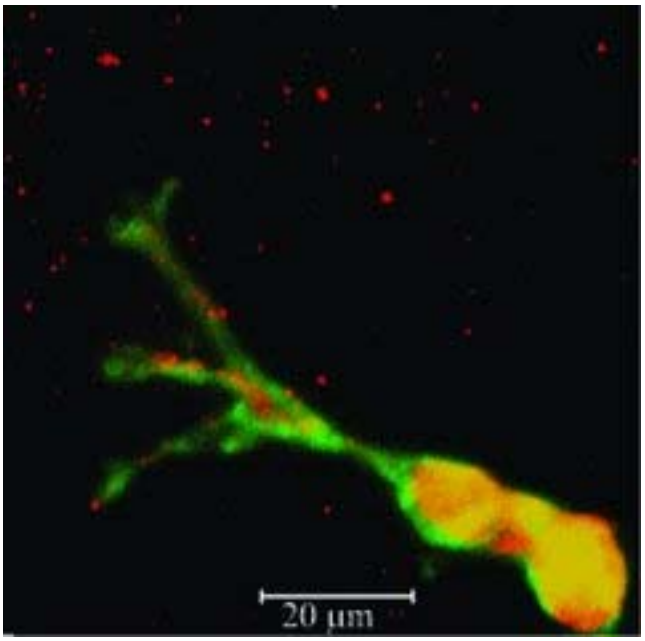

F**igure 7. Primary endothelial cells guided in 3D patterned agarose hydrogel**[93]. VEGF165 was immobilized in a concentration gradient within the scaffold using the thiol-maleimide click reaction.

The 'click' nature of thiol addition to a maleimide unit was also exercised by Kosif et al.[125] with the immobilization of proteins in PEG-methacrylate based hydrogels. Hydrogel synthesis was achieved using AIBN initiated thermal polymerization, by which they directly incorporated a furan-protected maleimide containing monomer. This furan-protected maleimide represents a DA adduct which is susceptible to thermal cycloreversion. Post-gelation, a thermal cycloreversion step activated the maleimide group to its thiol-reactive form. To evaluate this system as a potential template for bioconjugation, thiolated-biotin was covalently attached to the hydrogels, and its affinity for streptavidin investigated. This system is particularly intriguing as it incorporates the retro-DA click reaction, which is not commonly applied in regenerative biomaterials.

1.3 Thesis Objective

Current cross-linking chemistries for HA often require a coupling agent, catalyst, or photoinitiator, which may be cytotoxic, or involve a multistep synthesis of functionalized-HA, increasing the complexity of the system. With the goal of designing a simpler one-step, aqueous-based cross-linking system, we propose to synthesize HA hydrogels via Diels-Alder "click" chemistry. We have previously exploited this chemistry for conjugation of antibodies to nanoparticles for targeted drug delivery[76], and others have used it to create synthetic polymeric hydrogels[56-58]. A furan-modified HA derivative can be synthesized and subsequently cross-linked via dimaleimide PEG, and the mechanical and degradation properties of this hydrogel system can be controlled by varying the furan to maleimide molar ratio. These hydrogels will ultimately serve as scaffolds for tissue regeneration.

1.3.1 Hypothesis

The Diels-Alder click reaction can serve as an efficient cross-linking chemistry for the formation of HA hydrogels with tunable mechanical and degradation properties for tissue engineering applications.

1.3.2 Specific Aims

1) To demonstrate that HA can be cross-linked via Diels-Alder click chemistry.

2) To demonstrate Diels-Alder cross-linked hydrogels can be tuned in terms of their mechanical and degradation properties.

3) To demonstrate that Diels-Alder cross-linked hydrogels are cytocompatible.

2 Materials and Methods

2.1 Materials

Dried sodium hyaluronate (HA) (2.34×10^5 amu), was purchased from Lifecore Biomedical (Chaska, MN, USA). Bis-maleimido-poly(ethylene glycol) ($(MI)_2PEG$) (3.0×10^4 amu, n = 44) was purchased from RAPP Polymere GmbH (Germany). Furfurylamine (FA) was supplied by Acros Organics (Belgium). 4-(4,6-Dimethoxy-1,3,5-triazin-2-yl)-4-methylmorpholinium chloride (DMTMM), D_2O, and KBr were supplied by Aldrich Chemistry (St. Louis, MO, USA). 2-(N-morpholino)-ethanesulfonic acid (MES) buffer and hyaluronidase (Type IV-S, lyophilized powder, 2140 units/mg) were purchased from Sigma Life Sciences (St. Louis, MO, USA). Dulbecco's phosphate buffered saline (DPBS) was purchased from Multicell Technologies Inc. (Woonsocket, RI, USA). Dialysis membranes were purchased from Spectrum Laboratories Inc. (Rancho Dominguez, CA, USA). Human adenocarcinoma cells (MDA-MB-231) were purchased from ATCC (Manassas, VA) catalog number HTB-26.

2.2 Synthesis

2.2.1 Synthesis and Characterization of HA-Furan

Furan-modified HA (HA-furan) derivatives were synthesized by dissolving HA (0.40 g, 1.02 mmol) in 40 mL of MES buffer (100 mM, pH 5.5) to which DMTMM was added in 4 (1.13 g, 4.08 mmol), 2 (0.56 g, 2.04 mmol) or 1 (0.28 g, 1.02 mmol) molar ratio (relative to the –COOH groups in HA) and stirred for 10 minutes. Furfurylamine was then added dropwise in a 2 (188.8 μL, 2.04 mmol), 1 (94.4 μL, 1.02 mmol) or 0.5 (47.2 μL, 0.51 mmol) molar ratio (relative to the –COOH groups in HA). The reaction was conducted at room temperature for 24 h, and then dialyzed against distilled water for 3 days (M_w cutoff 12,000-14,000 Da). Water was completely removed by lyophilization to obtain HA-furan derivatives as a white powder. The degree of substitution (DS) was determined from ^{1}H NMR spectra by comparing the ratio of the areas under the proton peaks at 6.26, 6.46 and 7.65 ppm (furan protons) to the peak at 1.9 ppm (N-acetyl glucosamine protons of HA). ^{1}H NMR spectra were recorded in D_2O on a Varian Mercury-400 MHz NMR spectrometer (Palo Alto, CA, USA).

2.2.2 Synthesis of HA-PEG Hydrogels

HA-PEG hydrogels were synthesized by reacting HA-furan with commercial $(MI)_2$PEG cross-linker separately in MES buffer (100 mM, pH 5.5). The concentration of HA-furan was held constant at 1.5% w/v while the concentration of $(MI)_2$PEG was varied to examine differences in hydrogel properties as a function of the molar ratio of furans (HA-furan) to the molar ratio of maleimides ($(MI)_2$PEG). For example, 15 mg of HA-furan (DS 57.5%, 19.3 μmol of furan) was dissolved in 1 mL MES buffer. $(MI)_2$PEG was dissolved in MES buffer at different concentrations: either 14.48 mg (9.65 μmol of maleimide, Furan/MI 1:0.5), 28.95 mg (19.3 μmol of maleimide, Furan/MI 1:1), or 57.92 mg (38.6 μmol of maleimide, Furan/MI 1:2) in 375 μL of MES buffer. HA-furan and $(MI)_2$PEG solutions were combined and vortexed to ensure thorough mixing. Samples were allowed to gel at room temperature. The final concentration of HA-furan in the hydrogels was always 1.1% w/v whereas the total polymer concentration (HA + PEG) within the hydrogels was either 2.1% w/v (1Furan/0.5MI), 3.2% w/v (1Furan/1MI), or 5.3% w/v (1Furan/2MI). Herein, HA hydrogels are referenced according to the furan to maleimide molar ratios as: 1Furan/0.5MI, 1Furan/1MI or 1Furan/2MI.

2.3 In vitro Characterization of HA-PEG Hydrogels

2.3.1 FTIR Spectroscopy of HA-PEG Hydrogels

Fourier transform infrared (FTIR) spectra were recorded for HA, HA-furan, $(MI)_2$PEG and dry cross-linked HA-PEG hydrogels to characterize the -C=C- in the Diels-Alder adduct, indicating chemical cross-linking. Spectra were recorded with a Spectrum 1000 FT-IR spectrometer (Waltham, MA, USA), collecting 32 scans in the 400-4000 cm^{-1} range with a resolution of $2cm^{-1}$.

2.3.2 Rheological Characterization

The viscoelastic mechanical properties of the HA-PEG hydrogels were measured with an AR-1000 rheometer fitted with a 60 mm, 2° acrylic cone using parallel plate geometry (TA Instruments, New Castle, USA). Upon casting the hydrogels (1 mL), the upper plate was immediately lowered to a gap size of 20 μm. Hydrogels were allowed to cure overnight at 37 °C using an integrated Peltier plate before testing. A frequency sweep was conducted from 0.1 – 630 rad/s at 0.1% strain to determine the shear elastic modulus (G') of hydrogels following a stress

sweep test to confirm the frequency and strain were within the linear viscoelastic region. Sample evaporation was minimized using a solvent trap.

2.3.3 Equilibrium Swelling of HA-PEG Hydrogels

To examine swelling properties, cross-linked HA-PEG hydrogel samples (100 μL) were synthesized using MES buffer (100 mM, pH 5.5) in pre-weighed vials according to the above procedure and accurately weighed (M_0). Samples (n = 15) were then incubated in 1 mL of DPBS buffer (100 mM, pH 7.4) at 37 °C. At select time points, the swelling ratio was determined by measuring the mass (M_t), following removal of buffer, and gently drying the hydrogel surface with a tissue. Hydrogels were then replenished with fresh buffer. From these data, swelling ratios (M_t/M_0) were calculated, and the equilibrium swelling ratio was recorded when the mass of the gels no longer increased.

2.3.4 Degradation Assay

To determine the stability of the HA-PEG hydrogels, samples (100 μL) were synthesized in pre-weighed vials according to the above procedure and allowed to swell in DPBS (100, mM pH 7.4) for 24h at 37 °C, after which the mass of the samples were measured (M_s). Degradation experiments were performed using 50 U mL^{-1} hyaluronidase in DPBS at 37 °C. At selected time points, the supernatant was removed, hydrogels were weighed (M_t), and percent of hydrogel mass remaining relative to the original swollen mass was calculated (M_t/ M_s). Fresh buffer containing hyaluronidase was replaced in each sample at each time point. Degradation profiles were also recorded for hydrogels incubated in DPBS at 37 °C with no enzyme present as a negative control.

2.3.5 Cell Culture and Viability

Human epithelial cells (MDA-MB-231) were maintained (<6 passages) in plastic culture flasks in RPMI 1640 growth medium with 10% fetal bovine serum (FBS), 10 UI/mL penicillin, and 10 μg/mL streptomycin. HA-PEG hydrogels were prepared as described and 350 μL samples pipetted into sterile 4-well chamber slides (Lab-Tek, USA). Hydrogels were left overnight to ensure complete gelation and then washed with culture media prior to cell plating. Cells were plated on top of each gel at a density of 3.0×10^4 cells per well in medium and maintained in a

tissue culture incubator (37 ºC, 5% CO_2, 95% humidified). Medium was exchanged every 2-3 days for 14 days afterwhich images were captured with a Zeiss Axiovert S100 (Carl Zeiss MicroImaging GmBH, Germany) inverted microscope equipped with an X-Cite 120 fluorescence illumination system (EXFO, Ontario, Canada) and a CoolSNAP HQ digital camera (Photometrics, Tucson, AZ) using Image-Pro Plus software (Media Cybernetics, Silver Spring, MD, USA). To test cell viability, 14 day cultures were treated using the LIVE/DEAD® Cell Viability assay (Invitrogen, Carlsbrad, CA) as per the manufacturer's instructions. Three representative images were captured for each gel, and the number of live and dead cells recorded (n = 6 gels).

2.4 Statistical Analysis

All statistical analyses were performed using GraphPad Prism version 5.00 for Windows (GraphPad Software, San Diego California USA, www.graphpad.com). Differences among groups were assessed by one-way ANOVA with Bonferroni *post hoc* correction to identify statistical differences among three or more treatments. A p-value of ≤ 0.05 was set as the criteria for statistical significance. Graphs are annoted where p-values are represented as * ≤ 0.05, ** ≤ 0.01, or *** ≤ 0.001. All data are presented as mean ± standard deviation.

3 Results

3.1 Synthesis and Characterization of HA-furan

HA-furan derivates were prepared in a simple, one-step reaction by coupling furfurylamine to HA carboxylates using 4-(4,6-dimethoxy-1,3,5-triazin-2-yl)-4-methylmorpholinium chloride (DMTMM) reagent (**Scheme 3**). DMTMM has been recognized as a highly efficient activator of polysaccharide carboxyl groups in aqueous conditions, superior to traditional carbodiimide coupling[78]. Indeed, in a reaction with 1-[3-(dimethylamino)propyl]-3-ethylcarbodiimide hydrochloride (EDCI), the yield of immobilization of furfurylamine on HA was much lower than that using DMTMM (**Figure 9 and Figure S3**). The structure and degree of substitution were determined by ^{1}H NMR (**Figure 8**). Resonances at 6.26, 6.46, and 7.65 ppm verified the presence of furan protons, and their integrated ratios were compared to that of the N-acetyl glucosamine proton peak of native HA, appearing at 1.9 ppm. By varying the molar ratios of HA:Furfurylamine:DMTMM, variable degrees of substitution, defined as the number of furans per HA disaccharide repeat, were obtained. Molar ratios of 1:2:4, 1:1:2, and 1:0.5:1 yielded HA-furan with 75 ± 8% (n = 4), 61 ± 7% (n = 4), and 49 ± 6% (n = 9) degrees of substitution respectively (**Figure 9, Figure S1 and Figure S2**). For the remaining studies, HA-furan with a degree of substitution of 49% was employed, as lower substituted HA hydrogels have been shown to display higher cellular bioactivity[77].

Scheme 3. Synthesis of HA-furan

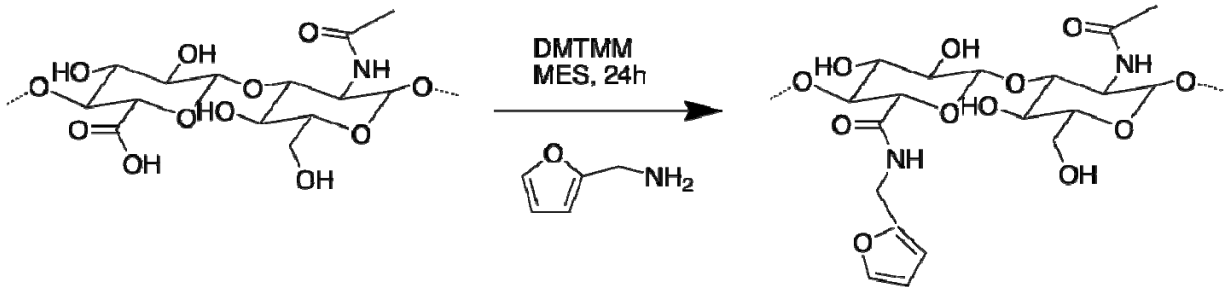

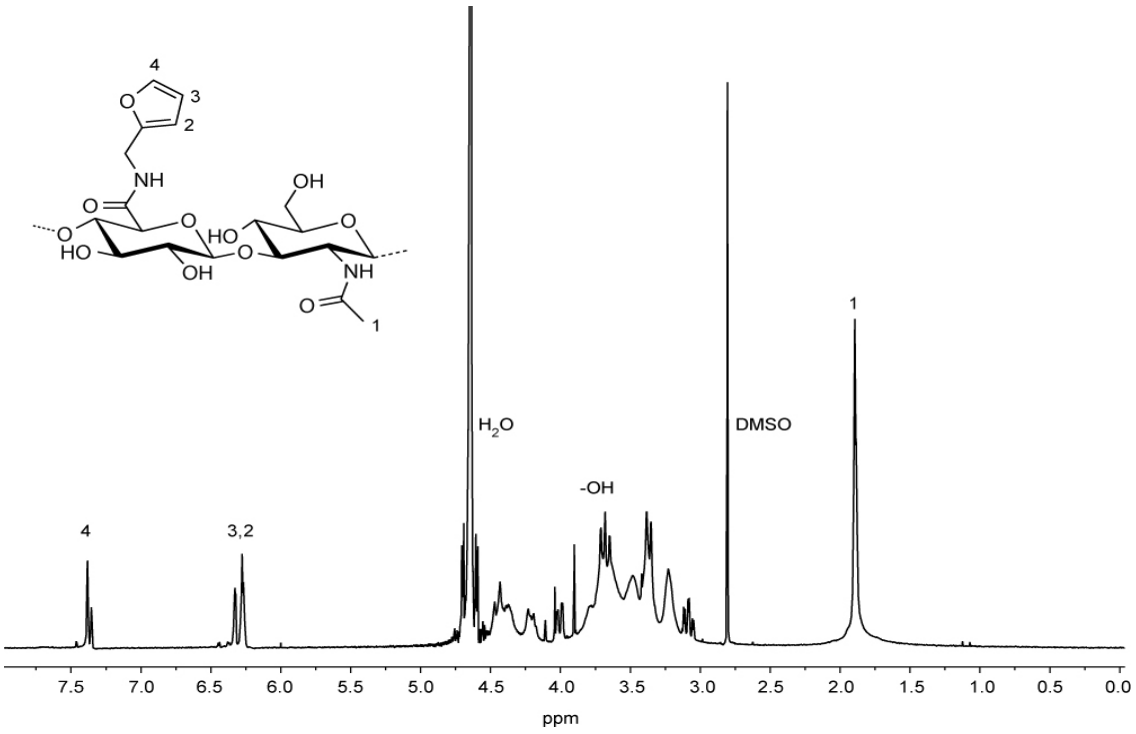

Figure 8. ^{1}H NMR spectra in D_2O (400 MHz) of HA-furan (DS = 54%). Degree of substitution was determined by comparing the integrated areas under the proton peaks at 6.26, 6.46, and 7.65 ppm (furan protons), indicated by 2,3, and 4 to that of the peak at 1.9 ppm (*N*-acetyl glucosamine of HA), indicated by 1.

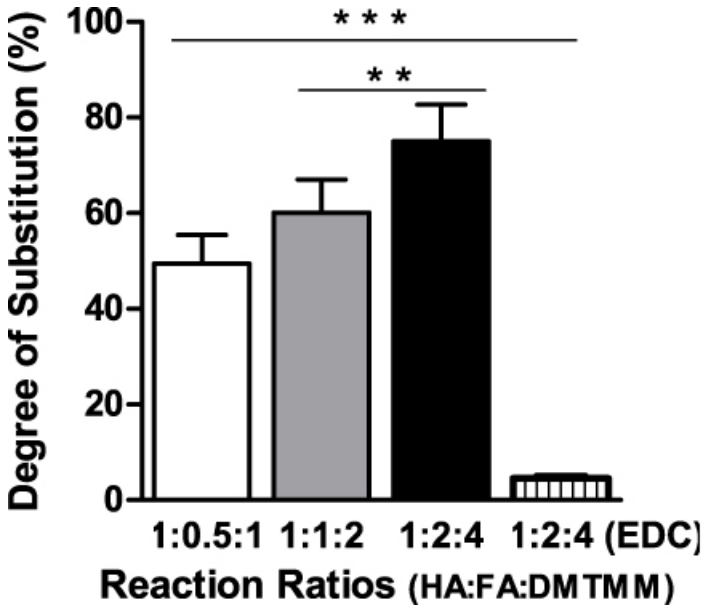

Figure 9. Controllable DS of HA-furan as determined by the molar reaction ratios. Increasing the molar ratio of furfurylamine (FA) and the coupling reagent DMTMM, relative to HA concentration, resulted in an increased degree of substitution. *Columns,* average degree of substitution, *Bars,* standard deviation (SD).

3.2 In vitro Characterization of HA-PEG Hydrogels

3.2.1 FTIR Characterization of HA-PEG Hydrogels

HA-PEG hydrogels were synthesized by mixing solutions of HA-furan and $(MI)_2$PEG cross-linker in MES buffer (pH 5.5) (**Scheme 4**). PEG was chosen as a cross-linker as it is often included in HA hydrogels to vary the mechanical properties and pore size of the scaffolds[65-68]. By controlling the chain length of the PEG cross-linker, one can control these properties. Incorporating a larger chain would result in a weaker gel with greater pore size, where as incorporating a smaller chain would result in a stiffer gel with smaller pores. As a preliminary step, PEG with a molecular weight of 3.0×10^4 amu was chosen. **Figure 10** displays FTIR spectra of HA, HA-furan, $(MI)_2$PEG and the cross-linked HA-PEG hydrogel. Conjugation of furfurylamine to the carboxylic acid on HA results in a shift of the C=O stretch on HA at 1617 cm^{-1} to 1653 cm^{-1}, characteristic of amide bond formation. Analysis of HA-furan and $(MI)_2$PEG spectra revels C=C peaks at 1455 cm^{-1} and 1466 cm^{-1} corresponding to the furan on HA-furan and the maleimide on $(MI)_2$PEG, respectively. Alkene bending is also quite apparent within the $(MI)_2$PEG spectrum with a sharp signal at 695 cm^{-1}, representing the C=C of the maleimide. The hydrogel spectrum shows decreased absorption of these C=C signals, and increased absorption at 1459 cm^{-1} (C=C in adduct) indicating the consumption of individual furan and maleimide groups and the formation of a maleimide-furan adduct during the Diels-Alder reaction.

Scheme 4. Synthesis of Diels-Alder cross-linked HA-PEG hydrogels

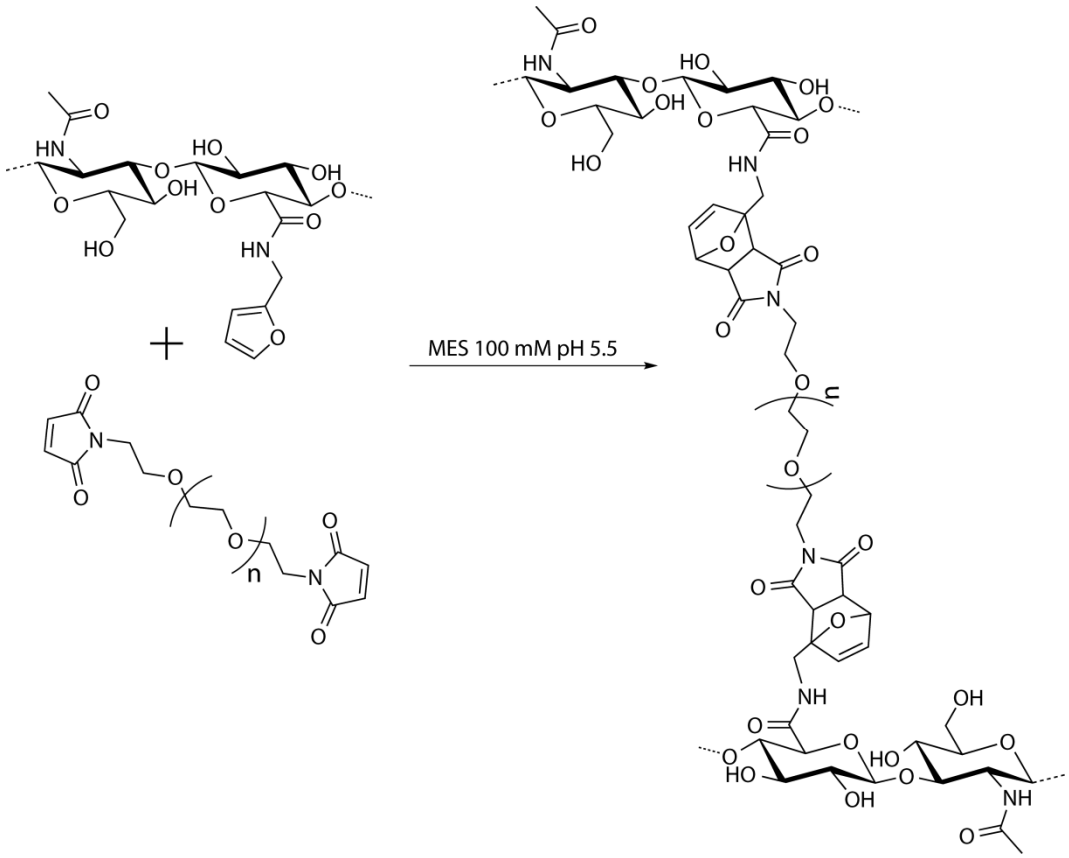

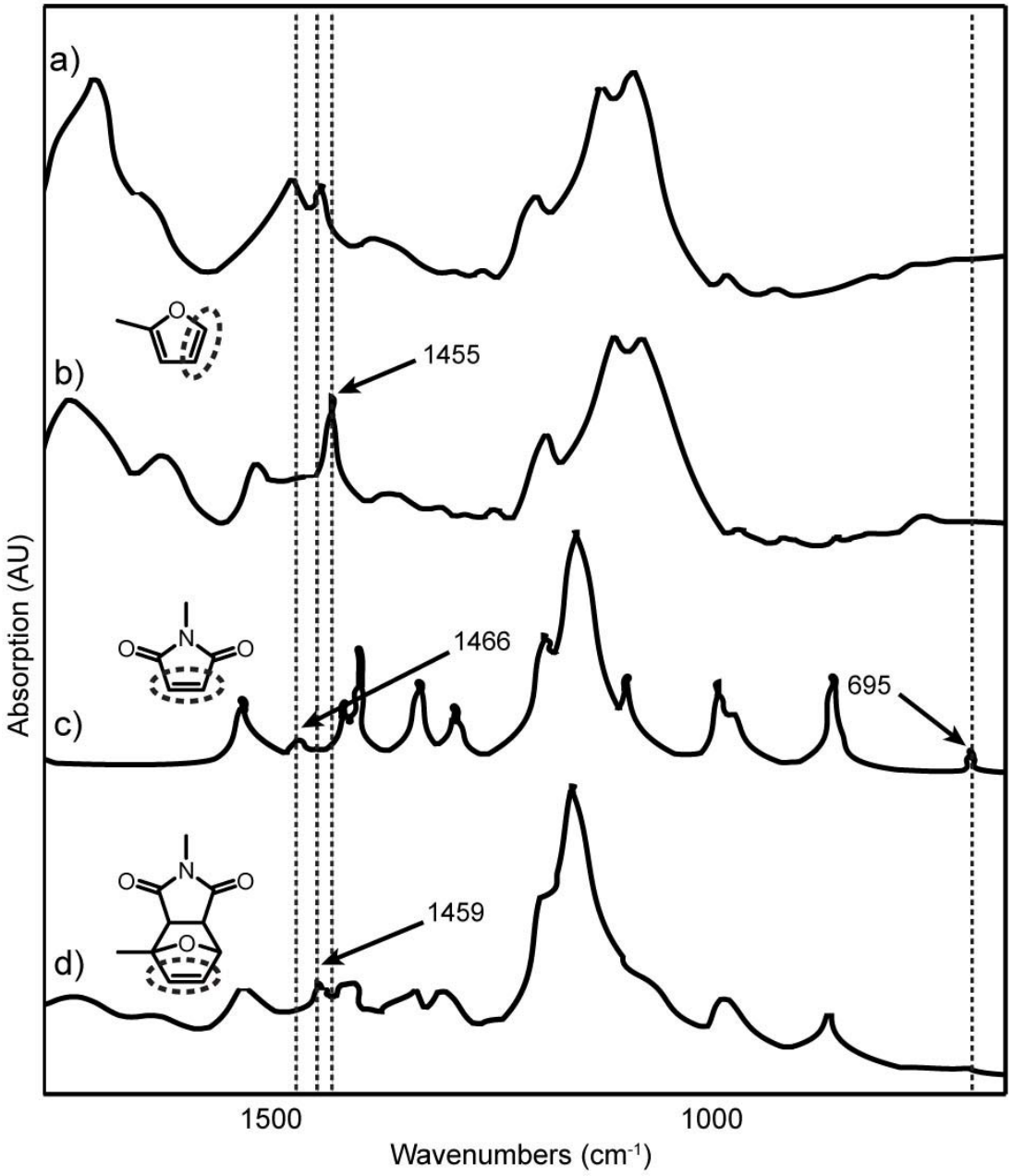

Figure 10. FTIR spectra of (a) HA, (b) HA-furan showing the C=C absorbance from furan at 1455 cm^{-1}, **(c) $(MI)_2$PEG** showing the C=C absorbance from maleimide at 1466 cm^{-1} and =C-H bending at 695 cm^{-1}, and **(d) cross-linked HA-PEG** showing a decrease in both the 695, 1455, and 1466 cm^{-1} peaks and the appearance of a new peak at 1459 cm^{-1} corresponding to the C=C bond in the Diels-Alder adduct.

3.2.2 Rheological Characterization of HA-PEG Hydrogels

The mechanical properties of HA-PEG hydrogels were characterized by oscillatory rheology studies using parallel plate geometry at 37 ºC. The aim of the rheological measurements was to characterize the G' value – the shear elastic modulus - for each HA-PEG hydrogel upon completion of the cross-linking reaction. In all cases, G' was independent of frequency, indicating hydrogels were cross-linked prior to recording measurements (**Figure 11**). Hydrogels were analyzed corresponding to their furan:maleimide (Furan/MI) ratio, that is, their cross-linker concentration. In all experiments the molar furan concentration was held constant while the molar maleimide concentration was varied. Cross-linker concentration was altered to distribute molar ratios of either 1Furan/1MI, 1Furan/0.5MI, or 1Furan/2MI within hydrogels. As shown in **Figure 12**, the elastic modulus of the hydrogels increased with higher cross-linker concentrations. There was significant difference between all hydrogel formulations ($p<0.001$) where increased maleimide concentrations resulted in higher cross-link density via the formation of additional Diels-Alder adducts. Accordingly, 1Furan/0.5MI hydrogels were the weakest with a G' value of 275 ± 54 Pa, while 1Furan/2MI hydrogels were the strongest with a G' value of 679 ± 62 Pa. The elastic modulus of 1Furan/1MI hydrogels was 557 ± 37 Pa, approximately double the strength of 1Furan/0.5MI hydrogels.

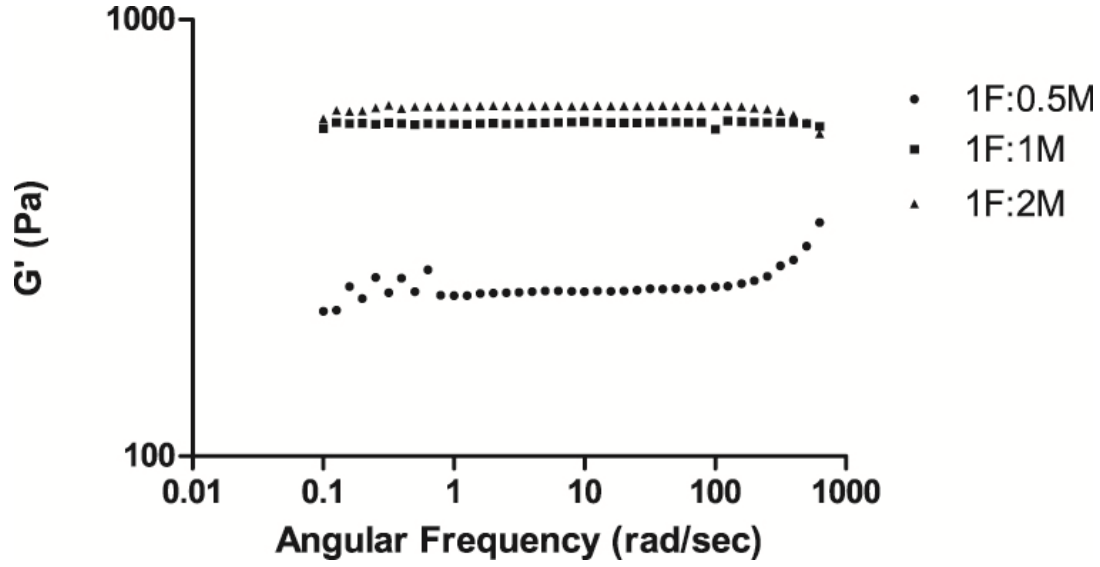

Figure 11. Representative frequency sweeps of HA-PEG hydrogels. The shear elastic modulus (G') was measured for each formulation of hydrogel. In all cases, G' was independent of frequency, indicating hydrogels were cross-linked prior to recording measurements.

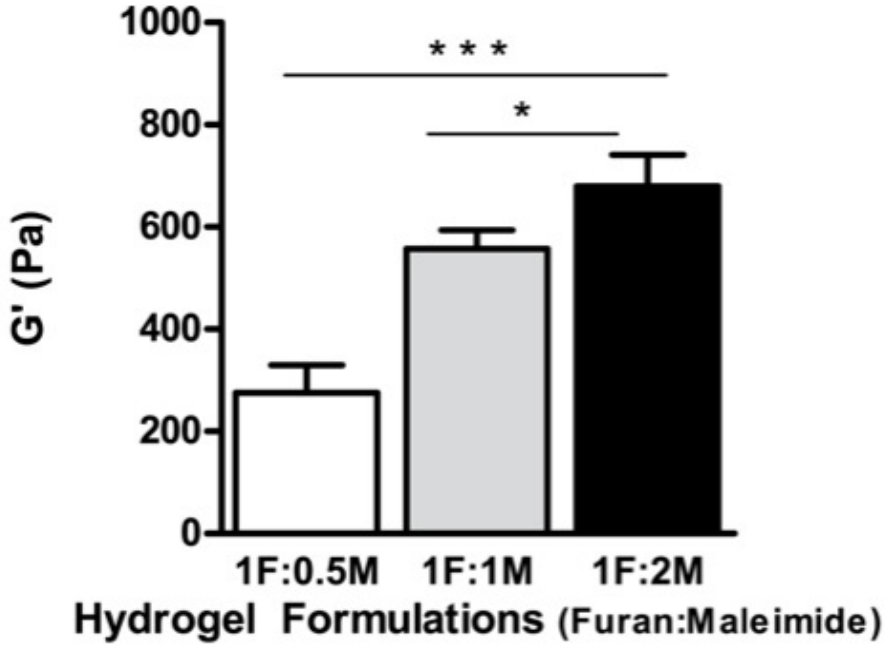

Figure 12. Rheological characterization of HA-PEG hydrogels. Increasing the concentration of cross-linker results in a stiffer gel. The difference between gels with a 1Furan/1MI ratio and a 1Furan/2MI ratio is not as great as that between 1Furan/0.5MI and 1Furan/1MI, suggesting efficient cross-linking (average elastic modulus ± standard deviation, $n = 4$).

3.2.3 Equilibrium Swelling

The swelling behavior of HA-PEG hydrogels was monitored by mass after incubation in DPBS at 37 ºC. Swelling ratios reached a plateau after 24 hours (**Figure 13**), and reported equilibrium swelling values are taken from this time point (**Table 1**). While the data is significantly different ($p<0.001$, $n = 15$), the values are effectively quite similar. 1Furan/0.5MI hydrogels swelled the most. Surprisingly, 1Furan/2MI hydrogels had a similar equilibrium swelling ratio to the 1Furan/0.5MI samples, and both were greater than that of 1Furan/1MI gels.

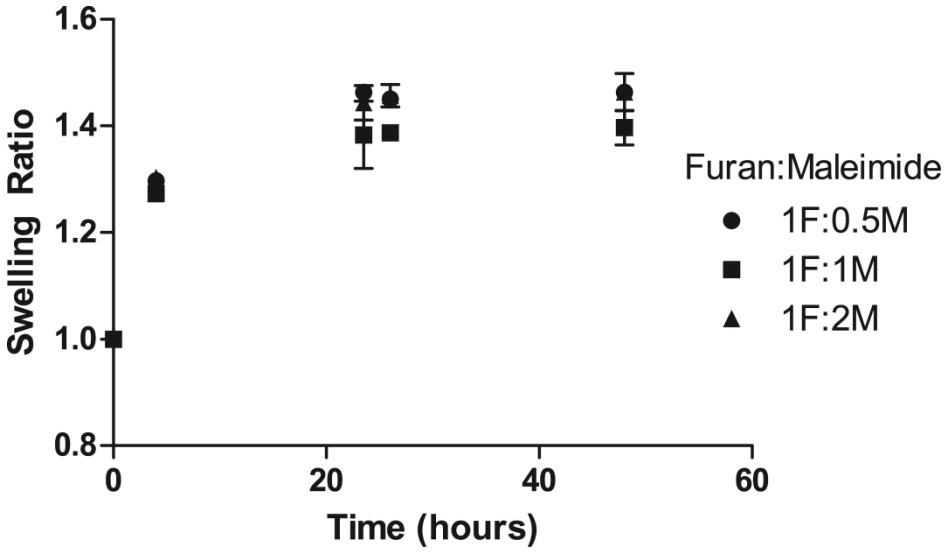

Figure 13. Equilibrium swelling with respect to time for HA-PEG hydrogels. The swelling behaviors of HA-Furan hydrogels were monitored after incubation in DPBS at 37ºC for designated times. Swelling ratios are defined as the ratio of weight at measured times, divided by the original weight of the sample. Swelling reached a plateau after 24 hours for all formulation. *Symbols,* average swelling ratio, *Bars,* standard deviation (SD), (n=15).

Table 1. Equilibrium swelling data (average ± standard deviation, $n = 15$)

Hydrogel Formulation	Equilibrium Swelling Ratio	$(MI)_2$PEG Concentration(% wt/v)
1Furan/0.5MI	1.48 ± 0.03	0.95
1Furan/1MI	1.39 ± 0.04	1.89
1Furan/2MI	1.44 ± 0.04	3.78

3.2.4 Degradation Assay

To monitor in vitro degradation of HA-PEG hydrogels, samples were incubated in DPBS with 50 U mL^{-1} of hyaluronidase versus PBS alone at 37 °C, and their masses were recorded over 52 hours. Samples incubated in PBS (controls) showed no significant mass loss after 52 hours, whereas samples incubated in hyaluronidase were completely degraded in this time frame (**Figure 14**). Degradation rates were calculated from the linear slope of the percentage of original mass versus time (**Figure 15**). Degradation rates directly correlated with cross-linker concentration, with 1Furan/0.5MI hydrogels degrading the fastest at 3.40 ± 0.19%/hour, and 1Furan/2MI hydrogels degrading the slowest at 2.06 ± 0.04%/hour. 1Furan/1MI hydrogels displayed an intermediate degradation profile at 2.23 ± 0.06%/hour. The degradation rate of 1Furan/0.5MI hydrogels was significantly greater compared to 1Furan/1MI and 1Furan/2MI hydrogels; however, there was no significant difference ($p > 0.05$) between 1Furan/1MI and 1Furan/2MI hydrogels.

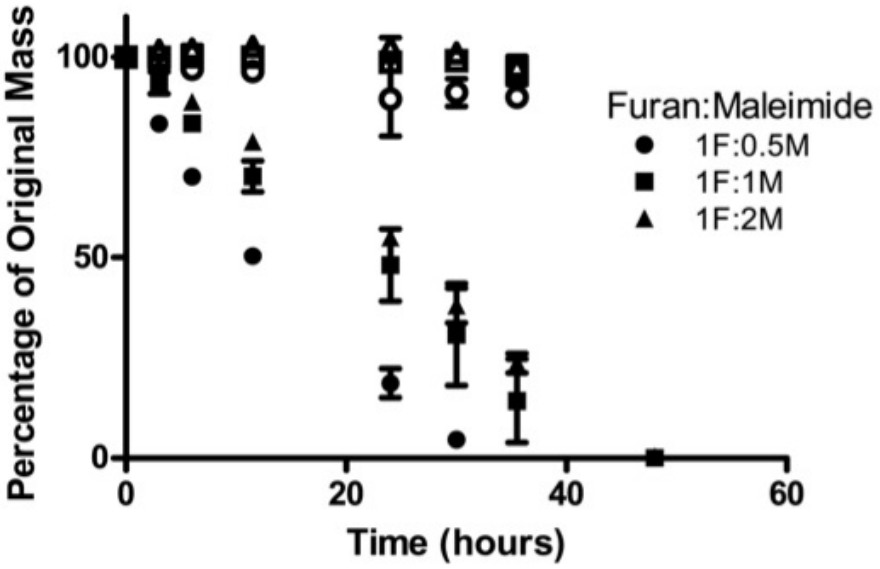

Figure 14. In vitro HA-PEG hydrogel degradation. Solid shapes: samples incubated in PBS with 50 U mL^{-1} of hyaluronidase. Open shapes: samples incubated in PBS (control) (average percentage of original weight ± standard deviation $n = 3$).

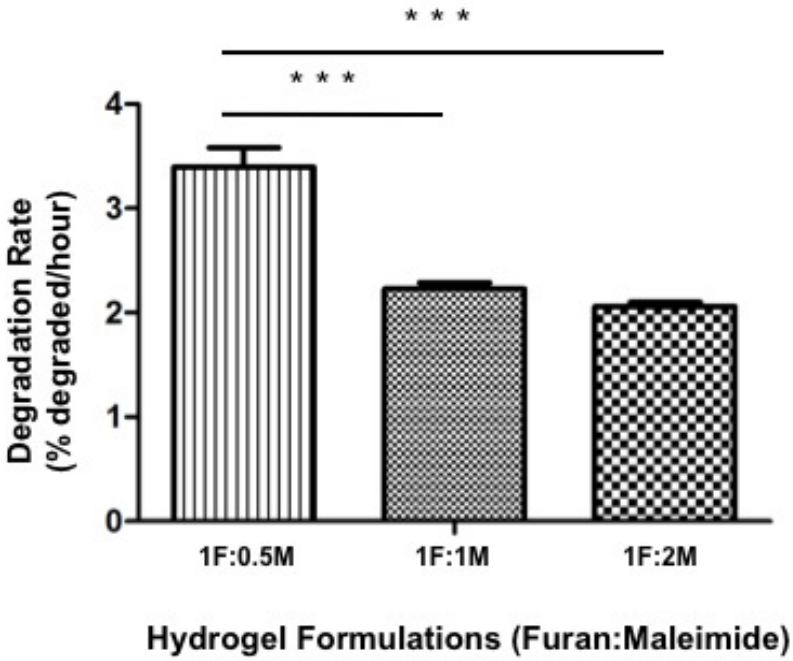

Figure 15. Degradation rate of HA-PEG hydrogels. Increasing the concentration of cross-linker results slower degradation rate. The difference between gels with a 1Furan/1MI ratio and a 1Furan/2MI ratio is not statistically significant, where as the difference between gels with a 1Furan/0.5MI and a 1Furan/1MI ratio is. (average elastic modulus ± standard deviation, $n = 3$).

3.2.5 Cell Attachment and Viability

The morphology and viability of endothelial cells was assessed after 14 days of culture in vitro. MDA-MB-231 cells were selected because they express CD44, the receptor for HA, allowing for cell interaction and potential adhesion to the HA-PEG hydrogels used in this study[84]. Cells plated on the hydrogels remained rounded for the first 24 hours, after which the majority of cells began to adopt a flattened morphology, suggesting cell attachment as shown in **Figure 16a**. Cells continued to spread, and remained attached to hydrogels for the duration of the experiment.

Cell viability was evaluated using a live/dead assay that stains live cells green (calcein AM) and dead cells red (ethidium homodimer). HA-PEG hydrogels showed a high level of cell survival (>98%) as seen in **Figure 16b**, demonstrating the cytocompatability of the hydrogels. It is important to note that a significant number of cells initially seeded onto hydrogels did not adhere to the gels, and were removed during media exchange. Nevertheless, several cells attached and proliferated, suggesting a CD44 interaction with HA. Indeed, when a cell line expressing low levels of CD44s was cultured on HA-PEG hydrogels, morphological characteristics indicative of attachment were not present (**Figure S4)**.

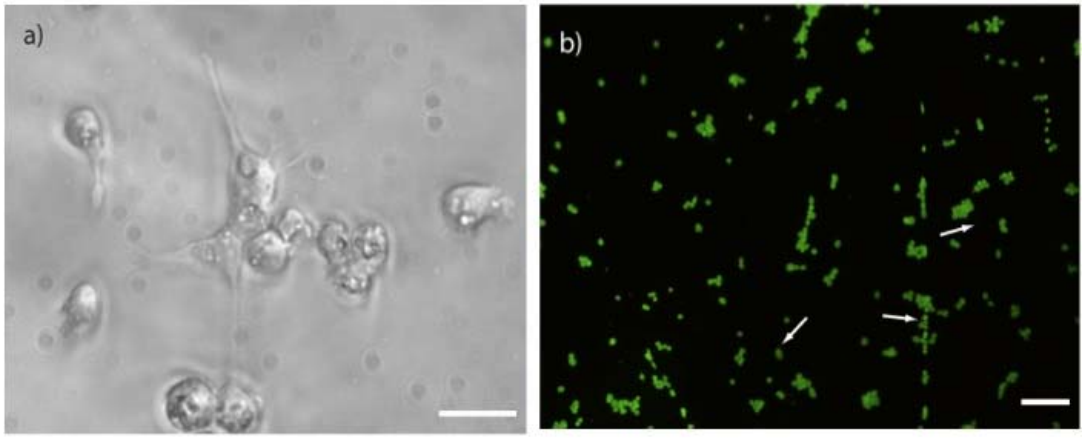

Figure 16. (a) Representative image of MDA-MB-231 cells grown on HA-PEG hydrogels for 14 days showing morphology characteristics of cell attachment (40X magnification, scale bar = 20 um). **(b) Live/dead assay** demonstrating the high level of cell survival (>98%). Live cells (green) and dead cells (red: indicated by arrows) are seen on hydrogels after 14 days in culture (10X magnification, scale bar = 60 um).

4 Discussion

4.1 Synthesis and Characterization of HA-furan

HA derivates are commonly synthesized using EDCI chemistry[31,94,95]. This requires a high excess of reagents with respect to HA (20 – 40 molar excess) due to the limited yield of amidation processes in aqueous media[96,97]. Bromoacetate-derivatized HA has been synthesized without the addition of a coupling agent[98], but requires basic conditions, which is not optimal for HA modification, and also requires a high molar excess due to competing side reactions. We have demonstrated the use of DMTMM as a coupling agent is superior for the synthesis of HA derivatives. Utilization of EDCI results in a considerable amount of undesired side reactions formed, contributing to lower reaction yields. Furthermore, DMTMM is more stable under aqueous conditions, optimal for HA modification[78]. We have also demonstrated control over the degree of substitution of HA-furan. This is beneficial as the mechanical properties and biodegradation of HA hydrogels can be tuned by varying the degree of substitution on the HA backbone[79].

4.2 In vitro Characterization of HA-PEG Hydrogels

4.2.1 FTIR Characterization of HA-PEG Hydrogels

The characteristic shift of the C=O on HA from 1617 to 1653 cm^{-1} confirms the conjugation of furan to the HA backbone, as determined by ^{1}H NMR. While it is difficult to accurately quantify any residual furan or maleimide groups on the individual polymers to estimate a degree of cross-linking, the appearance of this new signal on the FTIR spectra of the cross-linked hydrogel confirms covalent cross-linking.

4.2.2 Rheological Characterization of HA-PEG Hydrogels

In order to fully analyze the mechanical behavior of these hydrogels, the rubber elasticity theory must be introduced. This theory states that lightly cross-linked networks under uniaxial extension experience an elastic stress that is directly proportional to the number of network chains per unit volume[83]. Therefore, according to this theory, the mechanical behavior of a gel is largely

dependent on the architecture of the polymer network. Hence, by measuring the G' of a hydrogel, one can approximate the cross-link density of the network. Since G' increased from 1Furan/1MI to 1Furan/2MI, it is apparent the reaction between the furan and maleimide does not proceed to 100% conversion. However, the G' doubling effect between 1Furan/0.5MI and 1Furan/1MI, was not maintained between 1Furan/1MI and 1Furan/2MI, indicating G' reaches a plateau with an increased cross-linker concentration. These results confirm Diels-Alder click chemistry is efficient for the formation HA hydrogels.

In tissue engineering, it is important to consider the mechanical properties of the tissue of interest[78]. **Table 2** summarizes the shear moduli for tissues and culture substrates. The shear moduli of the HA-PEG hydrogels are similar to those of brain and nerve tissues (100 – 1000 Pa)[79], thus making them compelling scaffolds for neural tissue engineering. By varying other parameters, such as the degree of substitution, molecular weight, or concentration of HA-furan, the shear moduli may be further manipulated to mimic those of connective tissue, liver, and the mammary fat pad, among others. For example, the shear elastic moduli of liver, fat, relaxed muscle, and breast gland tissue range from 1000 – 10,000 Pa[80-82]. These values could be achieved by using a higher molecular weight HA or a higher HA weight concentration[79].

Table 2. Approximate shear moduli for tissues and culture substrates[79]

Material	**G' (Pa)**
Brain, nerves	$10^2 – 10^3$
Liver, fat, relaxed muscle, breast gland tissue	$10^3 – 10^4$
Dermis, connective tissue, contracted muscle	$10^5 – 10^6$
Eepidermis, cartilage	$10^7 – 10^8$
Polyacrylamide gels	$10^3 – 10^4$
Bone, polystyrene	$10^8 – 10^{10}$
Glass	10^{11}

4.2.3 Equilibrium Swelling

It is important to consider the swelling properties of a hydrogel, given that the degree of swelling is intimately related to the mechanical properties of a cross-linked network as dictated by the the rubber elasticity theory[83]. For a specific hydrogel, a higher degree of swelling coincides with a reduction in stress, or in other words, a decrease in cross-link density results in a decrease in stress. HA-PEG hydrogels, synthesized in MES buffer at pH 5.5, were expected to swell upon submersion in DPBS buffer at pH 7.4. The pH of the swelling buffer is greater than the pK_a of the carboxylic groups on the HA backbone (2.9)[86], causing dissociation of all the acidic groups. Even though the carboxylic groups on the native HA backbone were targeted during the synthesis of HA-furan (**Scheme 3**), the NMR spectrum (**Figure 8**) demonstrates only 49% of the carboxylic groups were modified, providing adequate carboxylic groups to allow swelling. In order to maintain electroneutrality, mobile ions from the external solution migrate into the gel, and through osmosis, the hydrogel swells[85].

As predicted, the 1Furan/0.5MI gels experienced the highest degree of swelling. This was expected as according to the rheological data, these samples have the lowest cross-link density of the three formulations. This is consistent with the rubber elasticity theory that degree of equilibrium swelling of a polymeric hydrogel being inversely proportional to its elastic modulus[83]. Interestingly, the 1Furan/2MI hydrogels displayed a higher equilibrium swelling ratio compared to the 1Furan/1MI hydrogels. This cannot be accounted for by the rubber elasticity theory, but by the polymer content of the hydrogel. The equilibrium swelling ratio of the 1Furan/0.5MI hydrogels has fewer cross-links, and thus swells more, whereas the 1Furan/2MI imbibes more water due to a greater concentration of PEG cross-linker.

4.2.4 Degradation Assay

The degradation profile of a hydrogel represents another important property, which relates to the mechanical properties of the network, and hence can be used to elucidate the cross-link density. Hydrogel degradation is largely attributed to hydrolysis of the either the covalent cross-links or of the polymer backbone through enzymatic degradation[87].

Statistical difference between the degradation rates was only observed when comparing the 1Furan/0.5MI gels compared to the other two formulations. There was no statistical difference

between the 1Furan/1MI and 1Furan/2MI hydrogels. These results suggest that the difference in the number of cross-links within 1Furan/1MI and 1Furan/2MI hydrogels did not impact degradation appreciably, revealing a degradation mechanism strictly dependent on HA enzymatic hydrolysis. The lower cross-link density of the 1Furan/0.5MI hydrogels permits facile diffusion of the enzyme within the hydrogel sample, enabling HA fragments to be released into solution at a faster rate. Furthermore, this data supports the conclusion derived from the rheological data that the 1Furan/2MI hydrogels possess the highest cross-link density.

Importantly, enzymatic recognition was retained with the furan-modification of HA, suggesting HA-PEG hydrogels are suitable for applications in tissue engineering. In vivo, predicted degradation rates for HA-PEG hydrogels would be much slower, as physiological hyaluronidase levels are much lower than that used in this study. While degradation was only monitored with respect to cross-linker concentration, varying the HA weight percent would expand the degradation profile[77].

4.2.5 Cell Attachment and Viability

MDA-MB-231 human endothelial cells were cultured on HA-PEG hydrogels for 14 days, adopting a flattened, adhesive morphology. These cells express a high level of CD44, the receptor for HA. When SKBR3 human epithelial cells were cultured on HA-PEG hydrogels, these morphological characteristics were not present. Importantly, with the furan modification on the HA backbone, cellular interaction with HA via the CD44 receptor was maintained. Moreover, these Diels-Alder cross-linked hydrogels were shown to be cytocompatible, and hence may represent a promising material for soft tissue engineering.

As mentioned in the introduction, HA hydrogels have been synthesized by another form of click chemistry – CuAAC. Crescenzi et al. synthesized azide and alkyne functionalized HA, which were then cross-linked upon the addition of CuCl[31]. In their study, they did not find the amount of Cu(I) to be toxic to yeast cells; however, they do state that for more advanced cell types, lower Cu(I) concentrations would be required. They propose to remove the catalyst through dialysis against EDTA solution. This however would cause undesirable effects on the mechanical properties of the hydrogel. Synthesis of HA hydrogels via Diels-Alder click chemistry

overcomes these hurdles, while simultaneously providing the efficient orthogonal cross-linking chemistry provided by CuAAC.

5 Conclusions

Diels-Alder chemistry is an effective cross-linking method to prepare hydrogels from furan-modified HA, and di-maleimide functionalized PEG. Synthesis of the scaffold backbone, HA-furan, was achieved in a single-step. Synthesis of the hydrogel required neither additional crosslinking agents, or catalysts, resulting in a clean, one-step synthetic procedure. The HA-PEG hydrogels had an elastic modulus similar to that of central nervous system tissue and demonstrated minimal swelling and complete degradation. Together with their cell-interactive properties, these HA-PEG hydrogels are likely suitable for applications in tissue engineering and regenerative medicine.

While the use of a click reaction for hydrogel cross-linking is not novel, this work reports the first use of Diels-Alder click chemistry for hydrogel formation, with a specific tissue engineering application in mind. The Diels-Alder click reaction is a "reagent-free" click reaction that does not require a catalyst, photoinitiator or radical initiation. Moreover, the Diels-Alder reaction is accelerated in aqueous solutions, an ideal characteristic for biomaterial design. Despite these strengths, the Diels-Alder click reaction has been much less explored relative to the CuAAC and thiol-ene click reactions, perhaps due to longer reaction times and the ability of Diels-Alder adducts to undergo cycloreversion. The latter is only relevant at higher temperatures, however, and thus should not pose a problem to biomaterials used in vivo.

In a short period of time, the use of click chemistry within the field of regenerative medicine has exploded. The ability to synthesize biomaterials with pristine definition and architecture to ultimately control drug delivery and stem cell fate is unprecedented. To this day, the click chemistry world continues to advance former click reactions while identifying new orthogonal chemistries. It is clear bioengineers will continue to translate these improved chemoselective methodologies to their biomaterials. Sequential click reactions will likely emerge as a key approach to design sophisticated biomaterials in a simplistic manner.

6 Recommendations and Future Directions

6.1 Determination of Cross-Link Density

From the presented data it was concluded the addition of additional $(MI)_2$PEG cross-linker resulted in a higher cross-link density, with 1Furan/0.5MI hydrogels displaying the lowest cross-link density, and 1Furan/2MI hydrogels displaying the highest cross-link density. However the actual cross-link density of the hydrogel samples was never determined. It is imperative to elucidate the hydrogel cross-link density as it can influence the cellular response in vito/and or in vivo. Furthermore, as determined from the swelling data, the rubber elasticity theory fails to accurately estimate the cross-link density for this system. The cross-link density could be investigated using ^{1}H HR-NMR[88]. By grafting molecules onto insoluble supports, sufficient rotational mobility can be achieved by swelling the support in a suitable solvent, providing a high-resolution characterization tool for macromonomers[89], and hydrogel synthesis[90]. This technique was utilized to determine the degree of cross-linking for HA hydrogels cross-linked via CuAAC[31].

6.2 Efficiency of the Diels-Alder Click Reaction

The Diels-Alder cycloaddition represents a highly efficient click reaction that is free from side reactions and by-products; however, in the presented study, the efficiency of the Diels-Alder click reaction was never determined. It was concluded the reaction between the furan and maleimide does not proceed to 100% conversion, given that the G' increases between the 1Furan/1MI and 1Furan/2MI hydrogel formulations. This could be investigated using a post-gel modification with both furan and maleimide functionalized chromophores to survey for any residual maleimide/furan functionality.

6.3 Synthesis of a Biomimetic Tissue Engineering Scaffold

While it is clear the efficiency of the Diels-Alder cross-linking reaction is not 100%, this does not represent a negative result. In fact, these residual furans can be hijacked for bulk immobilization of maleimide functionalized molecules. Maleimide GRGDS has been immobilized within the HA hydrogels, making the hydrogels more cell adhesive (**Figure S5**). Incorporation of additional ECM peptides is currently being studied.

6.4 3D Patterning of Click Cross-Linked HA Hydrogels

Ultimate control of cell fate in 3D can be achieved by controlling the mechanical properties and the degradation profile of the scaffold, as well as protein immobilization. 3D patterning of proteins in hydrogels is crucial for spatial control of cellular activities such as cell migration, differentiation and proliferation[38,91]. Previous work from our laboratory has demonstrated guidance of both neural stem cells[92] and endothelial cells[93] within 3D patterned agarose hydrogels. Notwithstanding these exciting results, agarose is limited with respect to cell penetration, and is non-biodegradable. As such, we sought to translate our patterning technology to our novel Diels-Alder cross-linked HA hydrogels where we could control the mechanical properties, the degradation profile, as well as protein immobilization. Controlled protein immobilization has been achieved in defined volumes using a pulsed infrared laser and photochemistry (**Figure S6**). The effect of these 3D patterns on the cellular response is currently under investigation.

References

1. Langer, R., and Vacanti, J.P. (1993) Tissue engineering. *Science 260*, 920-926.
2. George, J.H.S. (2009) Engineering of Fibrous Scaffolds for use in Regenerative Medicine. *PhD Thesis, Imperial College London*, London, UK.
3. Lee, K.Y., and Mooney, D.J. (2001) Hydrogels for Tissue Engineering. *Chem. Reviews 101*, 1869-1879.
4. Tibbitt, M.W., and Anseth, K.S. (2009) Hydrogels as Extracellular Matrix Mimics for 3D Cell Culture. *Biotechnol. Bioeng. 103*, 655-663.
5. Owen, S.C., and Shoichet, M.S. (2010) Design of three-dimensional biomimetic scaffolds. *J. Biomed. Mater. Res., Part A 94A*, 1321-1331.
6. Engler, A.J., Sen, S, Sweeney, H.L., and Discher, D.E. (2006) Matrix elasticity directs stem cell lineage specification. *Cell 126*, 677-689.
7. Paszek, M.J., Zahir, N., Johnson, K.R., Lakins, J.N., Rozenberg, G.I., Gefen, A., Reinhart-King, C.A., Margulies, S.S., Dembo, M., and Boettiger, D. (2005) Tensional homeostasis and the malignant phenotype. *Cancer cell 8*, 241-254.
8. Ulrich, T.A., Pardo, E.M.D., and Kumar, S. (2009) The mechanical rigidity of the extracellular matrix regulates the structure, molitity, and proliferation of glioma cells. *Cancer Res. 69*, 4167-4174.
9. Boontheekul, T., Hill, E.E., Kong, H.J., and Mooney, D.J. (2007) Regulating myoblast phenotype through controlled gel stiffness and degradation. *Tissue Eng 13*, 1431-1442.
10. Allison, D.D., and Grande-Allen, K.J. (2006) Review. Hyaluronan: a powerful tissue-engineering tool. *Tissue Eng. 12*, 2131-2140.
11. Kuo, J.W. (2006) Practical Aspects of Hyaluronan Based Medical Products. *CRC/Taylor & Francis, Boca Ranton*.
12. Goodison, S., Urquidi, V., and Tarin, D. (1999) CD44 cell adhesion molecules. *Mol Pathol. 52*, 189-196.
13. Laurent, T.C., and Fraser, J.R. (1986) The properties and turnover of hyaluronan. *Found. Symp. 124*, 9-29.
14. Burdick, J.A., Prestwich, G.D. (2011) Hyaluronic Acid Hydrogels for Biomedical Applications. *Adv. Mater. 23*, H41-H56.
15. Chung, C., Mesa, J., Randolph, M.A., Yaremchuk, M., and Burdick, J.A. (2006) Influence of gel properties on neocartilage formation by auricular chondrocytes photoencapsulated in hydaluronic acid networks. *J. Biomed. Mater. Res., Part A 77A*, 518-525.
16. Ifkovits, J.L., Tous, E., Minakawa, M., Morita, M., Robb, J.D., Koomalsingh, K.J., Gorman, J.H., Gorman, R.C., and Burdick, J.A. (2010) Injectable hydrogel properties influence infarct expansion and extent of postinfarction left ventricular remodeling in an ovine model. *Proc. Natl. Acad. Sci. USA 107*, 11507-11512.
17. Masters, K.S., Shah, D.N., Leinwand, L.A., and Anseth, K.S. (2004) Designing scaffolds for valvular interstitial cells: Cell adhesion and function on naturally derived materials. *J. Biomed. Mater. Res., Part A 71A*, 172-180.
18. Chung, C., and Burdick, J.A. (2009) Influence of Three-Dimensional Hyaluronic Acid Microenvironments on Mesenchymal Stem Cell Chondrogenesis. *Tissue Eng., 15*, 243-254.
19. Gerecht, S., Burdick, J.A., Ferreira, L.S., Townsend, S.A., Langer, R., and Vunjak-Novakovic, G. (2007) Hyaluronic acid hydrogel for controlled self-renewal and

differentiation of human embryonic stem cells. *Proc. Natl. Acad. Sci. USA 104*, 11298-11303.
20. Hennink, W.E., and van Nostrum, C.F. (2002) Novel crosslinking methods to design hydrogels. *Adv. Drug Delivery Rev. 54*, 13-36.
21. Kolb, H.C., Finn, M.G., and Sharpless, K.B. (2001) Click Chemistry: Diverse Chemical Function from a Few Good Reactions. *Angew. Chem. Int. Ed. 40*, 2004-2021.
22. van Dijk, M., Rijkers, D.T.S., Liskamp, R.M.J., van Nostrun, C.F., and Hennink, W.E. (2009) Synthesis and Applications of Biomedical and Pharmaceutical Polymers via Click Chemistry Methodologies. *Bioconjugate Chem. 20*, 2001-2016.
23. Huisgen, R. (1968) Cycloadditions – defintion, classification, and characterization. *Angew. Chem., Int. Ed. Engl. 7*, 321-328.
24. Tornoe, C.W.; Christensen, C.; Meldal, M. (2002) Peptidotriazoles on solid phase: [1,2,3]-triazoles by regiospecific copper(I)-catalyzed 1,3-dipolar cycloadditions of terminal alkynes to azides. *J. Org. Chem. 67*, 3057-3064.
25. Rostovtsev, V.V., Green, L.G., Fokin, V.V., and Sharpless, K.B. (2002) A stepwise Huisgen cycloaddition process: Copper(I)-catalyzed regioselective "ligation" of azides and terminal alkynes. *Angew. Chem., Int. Ed. 41,* 2596-2599.
26. Ossipov, D.A., and Hilborn, J. (2006) Poly(vinyl alcohol)-Based Hydrogels Formed by "Click Chemistry". *Macromolecules 39*, 1709-1718.
27. Malkoch, M., Vestberg, R., Gupta, N., Mespouille, L., Dubois, P., Mason, A.F., Hedrick, J.L, Liao, Q., Frank, C.W., Kingsbury, K., and Hawker, C.J. (2006) Synthesis of well-defined hydrogel networks using Click chemistry. *Chem. Commun.* 2774-2776.
28. D'Souza, S.E., Ginsberg, M.H., and Plow, E.F. (1991) Arginyl-glycyl-aspartic acid (RGD): a cell adhesion motif. *Trends Biochem. Sci. 16*, 246-250.
29. Liu, S.Q., Ee, P.L.R., Ke, C.Y., Hedrick, J.L., and Yang, Y.Y. (2009) Biodegradable poly(ethylene glycol)-peptide hydrogels with well-defined structure and properties for cell delivery. *Biomaterials 30*, 1453-1461.
30. Van Dijk, M., van Nostrum, C.F., Hennink, W.E., Rijkers, D.T.S., and Liskamp, R.M.J. (2010) Synthesis and Characterization of Enzymatically Biodegradable PEG and Peptide-Based Hydrogels Prepared by Click Chemistry. *Biomacromolecules 11*, 1608-1614.
31. Crescenzi, V., Cornelio, L., Di Meo, C., Nardecchia, S., and Lamanna, R. (2007) Novel Hydrogels via Click Chemistry: Synthesis and Potential Biomedical Applications. *Biomacromolecules 8*, 1844-1850.
32. Testa, G., Di Meo, C., Nardecchia, S., Capitani, D., Mannina, L., Lamanna, R., Barbetta, A., and Dentini, M. (2009) Influence of dialkyne structure on the properties of new click-gels based on hyaluronic acid. *Int. J. Pharm. 378*, 86-92.
33. Hu, X., Li, D., Zhou, F., and Gao, C. (2011) Biological hydrogel synthesized from hyaluronic acid, gelatin and chondroitin sulfate by click chemistry. *Acta Biomater. 7*, 1618-1626.
34. Becer, C.R., Hoogenboom, R., and Schubert, U.S. (2009) Click Chemistry beyond Metal-Catalyzed Cycloaddition. *Angew. Chem., Int. Ed. 48*, 4900-4908.
35. Agard, N.J., Prescher, J.A., and Bertozzi, C.R. (2004) A strain-promoted [3 + 2] azide-alkyne cycloaddition for covalent modification of biomolecules in living systems. *J. Am. Chem. Soc. 126*, 15046-15047.
36. Codelli, J.A., Baskin, J.M., Agard, N.J., and Bertozzi, C.R. (2008) Second-generation difluorinated cyclooctynes for cooper-free click chemistry. *J. Am. Chem. Soc. 130*, 11486-11493.

37. Baskin, J.M., Prescher, J.A., Laughlin, S.T., Agard, N.J., Chang, P.V., Miller, I.A., Lo, A., Codelli, J.A., and Bertozzi, C.R. (2007) Copper-free click chemistry for dynamic in vivo imaging. *Proc. Natl. Acad. Sci. U.S.A. 104*, 16793-16797.
38. DeForest, C.A., Polizzotti, B.D., and Anseth, K.S. (2009) Sequential click reactions for synthesizing and patterning three-dimensional cell microenvironments. *Nat. Mater. 8*, 659-664.
39. DeForest, C.A., Sims, E.A., and Anseth, K.S. (2010) Peptide-Functionalized Click Hydrogels with Independently Tunable Mechanics and Chemical Functionality for 3D Cell Culture. *Chem. Mater. 22*, 4783-4790.
40. Hoyle, C.E., and Bowman, C.N. (2010) Thiol-Ene Click Chemistry. *Angew. Chem., Int. Ed. 49*, 1540-1573.
41. Qui, B., Stefanos, S., Ma, J., Lalloo, A., Perry, B.A., Leibowitz, M.J., Sinko, P.J., and Stein, S. (2003) A hydrogel prepared by in situ crosslinking of a thiol-containing poly(ethylene glycol)-based copolymer: a new biomaterial for protein drug delivery. *Biomaterials 24*, 11-18.
42. Lutolf, M.P., Lauer-Fields, J.L., Schmoekel, H.G., Metters, A.T., Weber, F.E., Fields, G.B., and Hubbell, J.A. (2003) Synthetic matrix metalloproteinase-sensitive hydrogels for the conduction of tissue regeneration: Engineering cell-invasion characteristics. *Proc. Natl. Acad. Sci. USA 100*, 5413-5418.
43. Sternlicht, M.D., and Werb, Z. (2001) How matrix metalloproteinase's regulate cell behavior. *Annu. Rev. Dev. Biol. 17*, 463-516.
44. Chawla, K., Yu, T.-B., Liao, S.W., and Guan, Z. (2011) Biodegradable and Biocompatible Synthetic Saccharide-Peptide Hydrogels for Three-Dimensional Stem Cell Culture. *Biomacromolecules 12*, 560-567.
45. Hiemstra, C., van der Aa, L.J., Zhong, Z., Dijkstra, P.J., and Feijen, J. (2007) Rapidly in Situ-Forming Degradable Hydrogels from Dextran Thiols through Michael Addition. *Biomacromolecules 8*, 1548-1556.
46. Fairbanks, B.D., Schwartz, M.P., Halevi, A.E., Nuttelman, C.R., Bowman, C.N., and Anseth, K.S. (2009) A Versatile Synthetic Extracellular Matrix Mimic via Thiol-Norbornene Photopolymerization. *Adv. Mater. 21*, 5005-5010.
47. Anderson, S.B., Lin, C.-C., Kuntzler, D.V., and Anseth, K.S. (2011) The performance of human mesenchymal stem cells encapsulated in cell-degradable polymer-peptide hydrogels. *Biomaterials 32*, 3564-74.
48. Diels, O., and Alder, K. (1928) Synthesen in der hydroaromatischen Reihe. *Justus Liebigs Annalen der Chemie 460*, 98-122.
49. Otto, S., and Engberts, J.B. (2003) Hydrophobic interactions and chemical reactivity. *Org. Biomol. Chem. 1*, 2809-2820.
50. Rideout, D.C., and Breslow, R.J. (1980) Hydrophobic acceleration of Diels-Alder reactions. *J. Am. Chem. Soc. 102*, 7816-7817.
51. Gheneim, R., Perez-Berumen, C., and Gandini, A. (2002) Diels-Alder Reactions with Novel Polymeric Dienes and Dienophiles: Synthesis of Reversibly Crosslinked Elastomers. *Macromolecules 35*, 7246-7253.
52. Adzima, B.J., Aguirre, H.A., Kloxin, C.J., Scott, T.F., and Bowman, C.N. (2008) Rheological and Chemical Analysis of Reverse Gelation in a Covalently Crosslinked Diels-Alder Polymer Network. *Macromolecules 41*, 9112-9117.
53. Chen, X., Dam, M.A., Ono, K., Mal, A., Shen, H., Nutt, S.R., Sheran, K., and Wudl, F. (2002) A Thermally Re-mendable Crosslinked Polymeric Material. *Science 295*, 1698-1702.

54. Costanzo, P.J., Demaree, J.D., and Beyer, F.L. (2006) Controlling Dispersion and Migration of Particulate Additives with Block Copolymers and Diels-Alder Chemistry. *Langmuir 22*, 10251-10257.
55. Chujo, Y., Sada, K., and Saegusa, T. (1990) Reversible Gelation of Polyoxazoline by Means of Diels-Alder Reaction. *Macromolecules 23*, 2636-2641.
56. Wei, H.-L., Yang, Z., and Shen, Y.-M. (2009) Thermosensitive hydrogels synthesized by fast Diels-Alder reactions in water. *Polymer 50*, 2836-2840.
57. Wei, H.-L., Yang, J., Chu, H.-J., Yang, Z., Ma, C.-C., and Yao, K. (2011) Diels-Alder Reaction in Water for Straightforward Preparation of Thermoresponsive Hydrogels. *J. Appl. Polym. Sci. 120*, 974-980.
58. Wei, H.-L., Yang, Z., and Shen, Y.-M. (2009) Thermosensitive hydrogels synthesized by fast Diels-Alder reactions in water. *Polymer 50*, 2836-2840.
59. Nimmo, C.M., and Shoichet, M.S. (2011) Regenerative Biomaterials that "Click": Simple, Aqueous-Based Protocols for Hydrogel Synthesis, Surface Immobilization, and 3D Patterning. (Invided Review Paper) *Bioconjugate Chem.* In press.
60. Nimmo, C.M., Owen, S.C., and Shoichet, M.S. (2011) Diels-Alder Click Crosslinked Hyaluronic Acid Hydrogels for Tissue Engineering. *Biomacromolecules 12*, 824-830.
61. Termeer, C., Sleeman, J. P., and Simon, J. C. (2003) Hyaluronan – magic glue for the regulation of the immune response? *Trends Immunol. 24*, 112-114.
62. Gupta, D., Tator, C. H., and Shoichet, M. S. (2006) Fast-gelling injectable blend of hyaluronan and methylcellulose for intrathecal, localized delivery to the injured spinal cord. *Biomaterials 27*, 2370-9.
63. Baier Leach, J., Bivens, K. A., Patrick Jr, C. W., and Schmidt, C. E. (2003) Photocrosslinked hyaluronic acid hydrogels: natural, biodegradable tissue engineering scaffolds. *Biotechnol. Bioeng. 82*, 578-589.
64. Burdick, J. A., Chung, C., Jia, X., Randolph, M. A., and Langer, R. (2005) Controlled degradation and mechanical behavior of photopolymerized hyaluronic acid networks. *Biomacromolecules 6*, 386-91.
65. Jin, R., Teixeira, L. S. M., Krouwels, A., Dijkstra, P. J., van Blitterswijk, C. A., Karperien, M., and Feijen, J. (2010) Synthesis and characterization of hyaluronic acid-poly(ethylene glycol) hydrogels via Michael addition: An injectable biomaterial for cartilage repair. *Acta Biomater. 6*, 1968-1977.
66. Patterson, J., Siew, R., Herring, S. W., Lin, A. S. P., Guldberg, R., and Stayton, P. S. (2010) Hyaluronic acid hydrogels with controlled degradation properties for oriented bone regeneration. *Biomaterials 31*, 6772-6781.
67. Seidlits, S. K., Khaing, Z. Z., Petersen, R. R., Nickels, J. D., Vanscoy, J. E., Shear, J. B., and Schmidt, C. E. (2010) The effects of hyaluronic acid hydrogels with tunable mechanical properties on neural progenitor cell differentiation. *Biomaterials 31*, 3930-3940.
68. Shu, X. Z., Ghosh, K., Liu, Y. C., Palumbo, F. S., Luo, Y., Clark, R. A., and Prestwich, G. D. (2004) Attachment and spreading of fibroblasts on an RGD peptide-modified injectable hyaluronan hydrogel. *J. Biomed. Mater Res., Part A 68A*, 365-375.
69. Park, S. N., Park, J. C., Kim, H. O., Song, M. J., and Suh, H. (2002) Characterization of porous collagen/hyaluronic acid scaffold modified by 1-ethyl-3-(3-dimethylaminopropyl)carbodiimide cross-linking. *Biomaterials 23*, 1205-1212.
70. Kang, C. E., Poon, P. C., Tator, C. H., and Shoichet, M. S. (2009) A new paradigm for local and sustained release of therapeutic molecules to the injured spinal cord for neuroprotection and tissue repair. *Tissue Eng Part A 15*, 595-604.

71. Luo, Y., Kirker, K. R., and Prestwich, G. D. (2000) Cross-linked hyaluronic acid hydrogel films: new biomaterials for drug delivery. *J. Controlled Release 69*, 169-184.
72. Park, Y. D., Tirelli, N., and Hubbell, J. A. (2003) Photopolymerized hyaluronic acid-based hydrogels and interpenetrating networks. *Biomaterials 24*, 893-900.
73. Shu, X. Z., Liu, Y. C., Luo, Y., Roberts, M. C., and Prestwich, G. D. (2002) Disulfide cross-linked hyaluronan hydrogels. *Biomacromolecules 3*, 1304-1311.
74. Skalska, J., Brookes, P. S., Nadtochiy, S. M., Hilchey, S. P., Jordan, C. T., Guzman, M. L., Maggirwar, S. B., Briehl, M. M., and Bernstein, S. H., (2009) Modulation of cell surface protein free thiols: a potential novel mechanism of action of the sesquiterpene lactone parthenolide. *PLoS ONE 4,* e8115.
75. Shi, M., Wosnick, J. H., Ho, K., Keating, A., and Shoichet, M. S. (2007) Immuno-polymeric nanoparticles by Diels-Alder chemistry. *Angew Chem Int Ed Engl 46*, 6126-31.
76. Farkas, P., and Bystrický, S. (2007) Efficient activation of carboxyl polysaccharides for the preparation of conjugates. *Carbohydr. Polym. 68*, 187-190.
77. Eng, D., Caplan, M., Preul, M., and Panitch, A. (2010) Hyaluronan scaffolds: a balance between backbone functionalization and bioactivity. *Acta Biomater. 6*, 2407-2414.
78. Shoichet, M. S. (2010) Polymer Scaffolds for Biomaterials Applications. *Macromolecules 43*, 581-591.
79. Vanderhooft, J. L., Alcoutlabi, M, Magda, J.J., and Prestwich, G. D. (2009) Rheological Properties of Cross-Linked Hyaluronan-Gelatin Hydrogels for Tissue Engineering. *Macromol. Biosci 9*, 20-28.
80. Chen, E. J., Novakofski, J., Jenkins, W. K., and Obrien, W. D. (1996) Young's modulus measurements of soft tissues with application to elasticity imaging. *IEEE Trans. Ultrason. Ferroelectr. Freq. Control 43,* 191-194.
81. O'Hagan, J. J., and Samani, A. (2009) Measurement of the hyperelastic properties of 44 pat, hological ex vivo breast tissue samples. *Phys. Med. Biol. 54*, 2557-2569.
82. Discher, D. E., Mooney, D. J., and Zandstra, P. W. (2009) Growth factors, matrices, and forces combine and control stem cells. *Science 324*, 1673-1677.
83. Anseth, K. S., Bowman, C. N., and BrannonPeppas, L. (1996) Mechanical properties of hydrogels and their experimental determination. *Biomaterials 17*, 1647-1657.
84. Sheridan, C., Kishimoto, H., Fuchs, R. K., Mehrotra, S., Bhat-Nakshatri, P., Turner, C. H., Goulet, R., Jr., Badve, S., and Nakshatri, H. (2006) CD44+/CD24-breast canver cells exhibit enhanced invasive properties: an early step nevessary for metastasis. *Breast Cancer Res 8*, R59.
85. Marcombe, R., Cai, S., Hong, W., Zhao, X., Lapusta, Y., and Suo X. (2010) A theory of constrained swelling of a pH-sensitive hydrogel. *Soft Matter 6*, 784-793.
86. Malay, O., Bayraktar, O., and Batigun, A. (2007) Complex coacervation of silk fibroin and hyaluronic acid. *Int. J. Bio. Macro. 40*, 387-393.
87. Meyvis, T.K.L., De Smedt, S.C., and Demeester, J. (2000) Influence of the Degradation Mechanism of Hydrogels on Their Elastic and Swelling Properties during Degradation. *Macromolecules 33*, 4717-4725.
88. Van Vlierberghe, S., Fritzinger, B., Martins, J.C., and Dubruel, P. (2010) Hydrogel Network Formation Revised: High-Resolution Magic Angle Spinning Nuclear Magnetic Resonance as a Powerful Tool for Measuring Absolution Hydrogel Cross-Link Efficiencies. *Applied Spectroscopy 64*, 1176-1180.
89. Hamcerencu, M., Desbrieres, J., Popa, M., Khoukh, A., Riess, G. (2007) New unsaturated derivatives of Xanthan gum: Synthesis and characterization. *Polymer 48*, 1921-1929.

90. Annunziata, R., Franchini, J., Ranucci, E., and Ferruti, P. (2007) Structural characterization of poly(amidoamine) networks via high-resolution magic angle spinning NMR. *Magn. Reson. Chem. 45*, 51-58.
91. Lee, S.H., Moon, J.J., and West, J.L. (2008) Three-dimensional micropatterning of bioactive hydrogels via two-photon laser scanning photolithography for guided 3D cell migration. *Biomaterials 29*, 2962-2968.
92. Luo, Y., and Shoichet, M.S. (2004) A photolabile hydrogel for guided three-dimensional cell growth and migration. *Nature materials 3*, 249-253.
93. Aizawa, Y., Wylie, R., and Shoichet, M. (2010) Endothelial Cell Guidance in 3D Patterned Scaffolds. *Adv. Mater. 22*, 4831-4835.
94. Darr, A., and Calabro, A. (2009) Synthesis and characterization of tyramine-based Hyaluronan hydrogels. *J Mater. Sci: Mater Med 20*, 33-44.
95. Pouyani, T., and Prestwich, G.D. (1993) Functionalized Derivatives of Hyaluronic Acid Oligosaccharides: Drug Carries and Novel Biomaterials. *Bioconjugate Chem. 5*, 339-347.
96. Crescenzi, V., Francescangeli, A., Renier, D., and Bellini, D. (2002) New cross-linked and sulfated derivatives of partially deacetylated hyaluronan: Synthesis and preliminary characterization. *Biopolymers 64*, 86-94.
97. Di Meo, C., Capitani, D., Mannina, L., Brancaleoni, E., Galesso, D., De Luca G., and Crescenzi, V. (2006) Synthesis and NMR Characterization of New Hyaluronan-Based NO Donors. *Biomacromolecules 7*, 1253-1260.
98. Serban, M.A., and Prestwich, G.D. (2007) Synthesis of Hyaluronan Haloacetates and Biology of Novel Cross-Linker-Free Synthetic Extracellular Matrix Hydrogels. *Biomacromolecules 8*, 2821-2828.
99. Musoke-Zawedde, P., and Shoichet, M.S. (2006) Anisotropic three-dimensional peptide channels guide neurite outgrowth within a biodegradable hydrogel matrix. *Biomed. Mater. 1*, 162-169.
100. Wosnick, J.H., and Shoichet, M.S. (2008) Three-dimensional Chemical Patterning of Transparent Hydrogels. *Chem. Mater. 20*, 55-60.
101. Adzima, B.J., Tao, Y., Kloxin, C.J., DeForest, C.A., Anseth, K.S., and Bowman, C.N. (2011) Spatial and temporal control of the alkyne-azide cycloaddition by photoinitiated Cu(II) reduction. *Nat. Chem. 3*, 258-261.
102. Wang, J.-S., and Matyjaszewski, K. (1995) 'Living'/controlled radical polymerization. Transition-metal-catalyzed atom transfer radical polymerization in the presence of a conventional radical initiator. *Macromolecules 28*, 7572-7573.
103. Hudalla, G.A., Murphy, W.L. (2009) Using "click" chemistry to prepare SAM substrates to study stem cell adhesion. *Langmuir 25*, 5737-5746.
104. Roberts, C., Chen, C.S., Mrksich, M., Martichonok, V., Ingber, D.E., Whitesides, G.M., (1998) Using mixed self-assembled monolayers presenting RGD and (EG)3OH groups to characterize long-term attachement of bovine capillary endothelial cells to surfaces. *J. Am. Chem. Soc. 120*, 6548-6555.
105. Arnold, M., Cavalcanti-Adam, E.A., Glass, R., Blummel, J., Eck, W., Kantlehner, M., Kessler, H., Spatz, J.P. (2004) Activation of Integrin Function by Nanopatterned Adhesive Interfaces. *ChemPhysChem 5*, 383-388.
106. Koepsel, J.T., Murphy, W.L. (2009) Patterning Discrete Stem Cell Culture Environments via Localized Self-Assembled Monolayer Replacement. *Langmuir 25*, 12825-12834.

107. Lahiri, J., Isaacs, L., Tien, J., Whitesides, G.M. (1999) A Strategy for the Generation of Surfaces Presenting Ligands for Studies of Binding Based on an Active Ester as a Common Reactive Intermediate: A Surface Plasmon Resonance Study. *Anal. Chem. 71*, 777-790.
108. Houseman, B.T., Gawalt, E.S., Mrksich, M. (2003) Maleimide-Functionalized Self-Assembled Monolayers for the Preparation of Peptide and Carbohydrate Biochips. *Langmuir 19*, 1522-1531.
109. Nebhani, L., and Barner-Kowollik, C. (2009) Orthogonal Transformations on Solid Substrates: Efficient Avenues to Surface Modification. *Adv. Mater. 21*, 3442-3468.
110. Gallant, N.D., Lavery, K.A., Amis, E.J., and Becker, M.L. (2007) Universal Gradient Substrates for "Click" Biofunctionalization. *Adv. Mater. 19*, 965-969.
111. Lu, J., Shi, M., and Shoichet, M.S. (2009) Click chemistry functionalized polymeric nanoparticles target corneal epithelial cells through RGD-cell surface receptors. *Bioconjugate Chem. 20*, 87-94.
112. Moore, N.M., Lin, N.J., Gallant, N.D., and Becker, M.L. (2010) The use of immobilized osteogenic growth peptide on gradient substrates synthesized via click chemistry to enhance MC3T3-E1 osteoblast proliferation. *Biomaterials 31*, 1604-1611.
113. Gabet, Y., Muller, R., Regev, E., Sela, J., Shteyer, A., Salisbury, K., Chorev, M., and Bab, I. (2004) Osteogenic growth peptide modulates fracture callus structural and mechanical properties. *Bone 35*, 65-73.
114. Chan, T.R., Hilgraf, R., Sharpless, K.B., and Fokin, V.V. (2004) Polytrizaoles as Copper(I)-Stabilizing Ligands in Catalysis. *Org. Lett. 6*, 2853-2855.
115. Hudalla, G.A., and Murphy, W.L. (2010) Immobilization of Peptides with Distinct Biological Activities onto Stem Cell Culture Substrates Using Orthogonal Chemistries. *Langmuir 26*, 6449-6456.
116. Yousaf, M.N., and Mrksich, M. (1999) Diels-Alder Reaction for the Selective Immobilization of Protein to Electroactive Self-Assembled Monolayers. *J. Am. Chem. Soc. 121*, 4286-4287.
117. Sun, X.-L., Stabler, C.L., Cazalis, C.S., and Chaikof, E.L. (2006) Carbohydrate and Protein Immobilization onto Solid Surfaces by Sequential Diels-Alder and Azide-Alkyne Cycloadditions. *Bioconjugate Chem. 17*, 52-57.
118. Jonkheijm, P., Weinrich, D., Kohn, M., Engelkamp, H., Christianen, P.C.M., Kuhlmann, J., Mann, J.C., Nusse, D., Schroeder, H., Wacher, R., Breinbauer, R., Niemeyer, C.M., and Waldmann, H. (2008) Photochemical Surface Patterning by the Thiol-Ene Reaction. *Angew Chem. 120*, 4493-4496.
119. Weinrich, D., Lin, P.-C., Jonkheijm, P., Nguyen, U.T.T., Schroder, H., Niemeyer, C.M., Alexandrov, K., Goody, R., and Waldmann, H. (2010) Oriented Immobilization of Farnesylated Proteins by the Thiol-Ene Reaction. *Angew. Chem., Int. Ed. 49*, 1252-1257.
120. Hightower, K.E., and Fierk, C.A. (1999) Zing-catalyzed sulfur alkylation: insights from protein farnesyltransferase. *Curr. Opin. Chem. Biol. 3*, 176-181.
121. Aizawa, Y., Leipzig, N., Zahir, T., and Shoichet, M. (2008) The effect of immobilized platelet derived growth factor AA on neural stem/progenitor cell differentiation on cell-adhesive hydrogels. *Biomaterials 29*, 4676-4683.
122. Rahman, N., Purpura, K.A., Wylie, R.G., Zandstra, P.W., and Shoichet, M.S. (2010) The use of vascular endothelial growth factor functionalized agarose to guide pluripotent stem cell aggregates toward blood progenitor cells. *Biomaterials 31*, 8262-8270.

123. Leipzig, N.D., Xu, C., Zahir, T., and Shoichet, M.S. (2010) Functional immobilization of interferon-gamma induces neuronal differentiation of neural stem cells. *Biomed. Mater. Res. A 93*, 625-633.
124. Polizzotti, B.D., Fairbanks, B.D., Anseth, K.S. (2008) Three-Dimensional Biochemical Patterning of Click-Based Composite Hydrogels via Thiolene Photopolymerization. *Biomacromolecules 9*, 1084-1087.
125. Kosif, I., Park, Eun-Ju, P., Sanyal, R., and Sanyal, A. (2010) Fabrication of Maleimide Containing Thiol Reactive Hydrogels via Diels-Alder/Retro-Diels-Alder Strategy. *Macromolecules 43*, 4140-4148.

Additional Figures

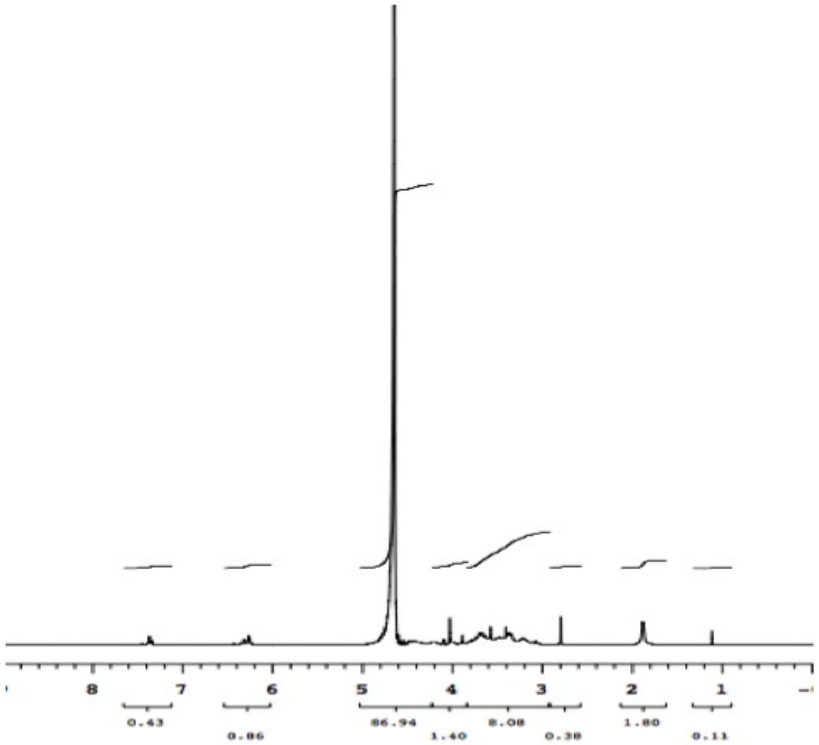

Figure S1. **^{1}H NMR spectra in D_2O (400 MHz) of HA-furan (HA:FA:DMTMM 1:1:2)**

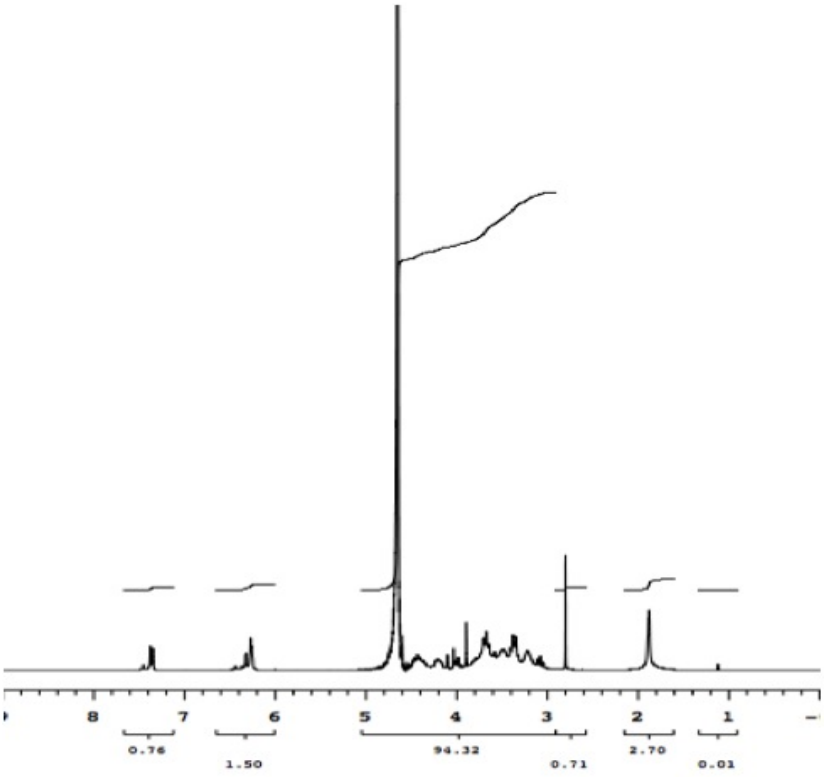

Figure S2. **^{1}H NMR spectra in D_2O (400 MHz) of HA-furan (HA:FA:DMTMM 1:2:4)**

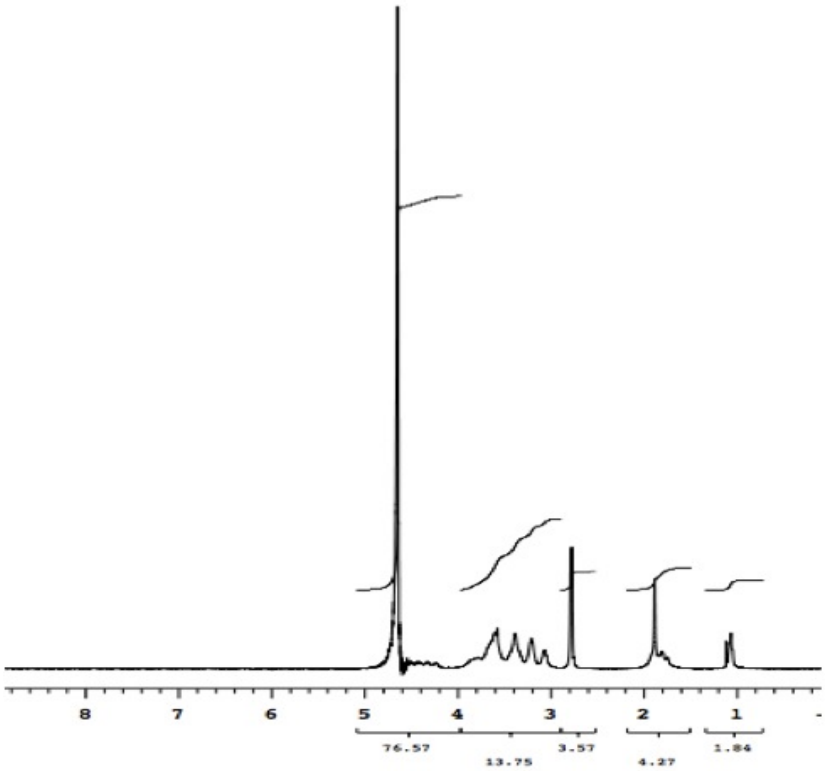

Figure S3. **^{1}H NMR spectra in D_2O (400 MHz) of HA-furan (HA:FA:EDC 1:2:4)**

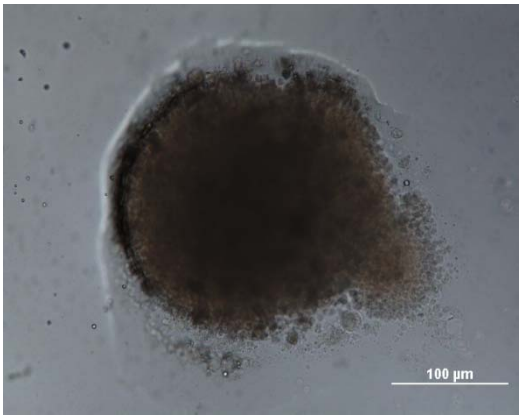

Figure S4. SKBR3 human epithelial cells grown on HA-PEG hydrogels. Cells did not adopt a flattened morphology compared to MDA-MB-231 cells, suggesting MDA-MB-231 cells are in fact interacting with the matrix through CD44 interaction.

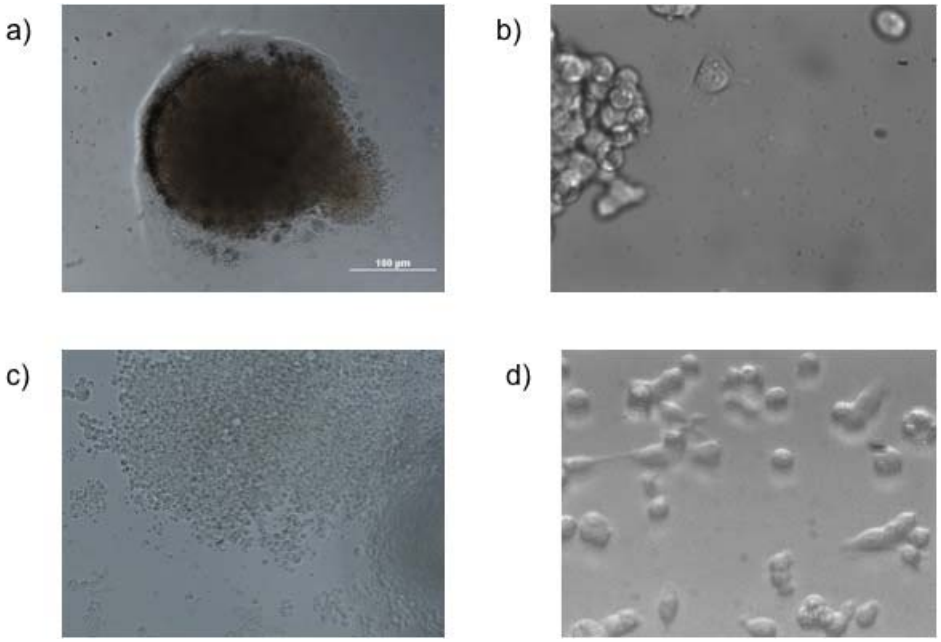

Figure S5. Cells cultured on HA-PEG hydrogels after RGD modification. a) MCF-7 cells cultured on native hydrogel **b)** MDA-MB-231 cells cultured on native hydrogel **c)** MCF-7 cells cultured on hydrogel after RGD modification **d)** MDA-MB-231 cells cultured on hydrogel after RGD modification. Incorporation of adhesive peptides enhances cellular interactions with the matrix.

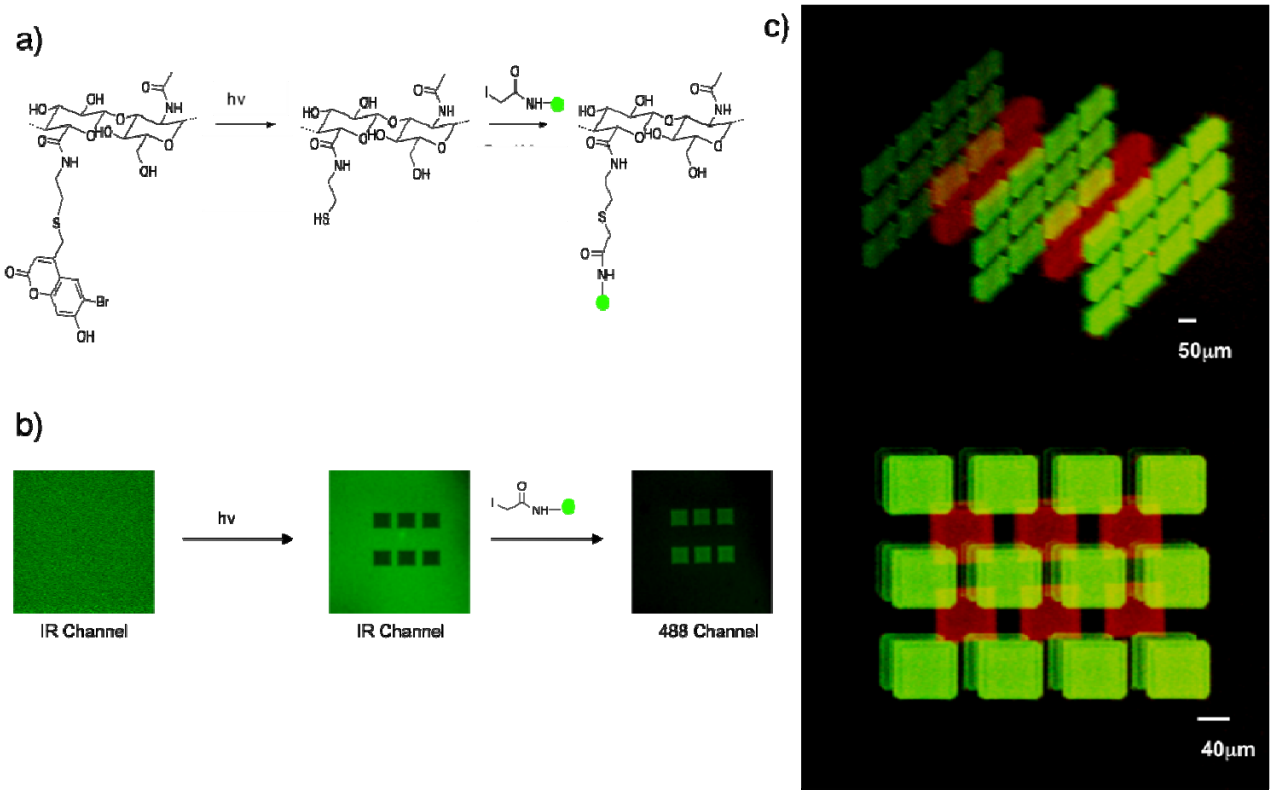

Figure S6. 3D patterning of HA hydrogels. a) HA hydrogels are exposed to two-photon excitation in 3D space, generating a pattern of free thiols, which in turn, react with iodoacetamide functionalized biomolecules. **b)** Confocal micrograph of coumarin sulfide HA hydrogel demonstrating loss of fluorescence following multiphoton irradiation in the IR channel and immobilization of 5-IAF in the 488 channel. **c)** A two-molecule pattern. Oblique (top micrograph) and side (bottom micrograph) views of a 4 x 4 x 3 array of 3D patterned squares (60 μm per side) of 5-IAF, over-patterned with a second 3 x 3 x 2 array of squares (60 μm per side) of 5-TMRIA.

Copyright Acknowledgements

Sections of the introduction and conclusion were adapted from an accepted review article to be published in Bioconjugate Chemistry with Chelsea Nimmo as the first author, and Molly S. Shoichet as co-author[59]. Proper copyright permission was granted from the American Chemical Society.

Chapter 2 was adapted from a published original research article in Biomacromolecules with Chelsea Nimmo as the first author, and Shawn C. Owen and Molly S. Shoichet as co-authors[60]. Proper copyright permission was granted from the American Chemical Society.